Penta, R., Ambrosi, D. and Quarteroni, A. (2015) Multiscale homogenization for fluid and drug transport in vascularized malignant tissues. Mathematical Models and Methods in Applied Sciences, 25(1), pp. 79-108.

MULTISCALE HOMOGENIZATION FOR FLUID AND DRUG TRANSPORT IN VASCULARIZED MALIGNANT TISSUES

R. PENTA

MOX, Dipartimento di Matematica, Politecnico di Milano
Piazza Leonardo da Vinci 32, Milano, 20133, Italy
raimondo.penta@polimi.it

D. AMBROSI *

MOX, Dipartimento di Matematica, Politecnico di Milano
Piazza Leonardo da Vinci 32, Milano, 20133, Italy
davide.ambrosi@polimi.it

A. QUARTERONI

Modeling and Scientific Computing, IACS-CMCS
Ecole Polytechnique Federale de Lausanne
Station 8, CH-1015, Lausanne, Switzerland
alfio.quarteroni@epfl.ch

A system of differential equations for coupled fluid and drug transport in vascularized (malignant) tissues is derived by a multiscale expansion. We start from mass and momentum balance equations, stated in the physical domain, geometrically characterized by the intercapillary distance (the *microscale*). The Kedem-Katchalsky equations are used to account for blood and drug exchange across the capillary walls. The multiscale technique (*homogenization*) is used to formulate continuum equations describing the coupling of fluid and drug transport on the tumor length scale (the *macroscale*), under the assumption of local periodicity; macroscale variations of the microstructure account for spatial heterogeneities of the angiogenic capillary network. A double porous medium model for the fluid dynamics in the tumor is obtained, where the drug dynamics is represented by a double advection-diffusion-reaction model. The homogenized equations are straightforward to approximate, as the role of the vascular geometry is recovered at an average level by solving standard cell differential problems. Fluid and drug fluxes now read as effective mass sources in the macroscale model, which upscale the interplay between blood and drug dynamics on the tissue scale. We aim to provide a theoretical setting for a better understanding of the design of effective anti-cancer therapies.

Keywords: Multiscale expansion; Homogenization; Tumor vasculature; Kedem-

---

* Corresponding author

Katchalsky equations.

AMS Subject Classification: 22E46, 53C35, 57S20

1. Introduction

During the early stage of tumor growth (the "avascular phase"), nutrients enter the malignant mass and feed its development by simple diffusion. When the size of the tumor exceeds the diffusion length scale, the angiogenetic process starts: new vessels sprout from the neoplastic mass and create an *ad hoc* supply network [8]. The new microvasculature is characterized by abnormal features, as regards both geometry and functionalities. Differently than healthy vessels, the tumor ones are disorganized, tortuous and dilated, while the vessels walls are highly permeable and exhibit openings and defects [14]. The tumor cells environment is often characterized by a high interstitial fluid pressure [22, 6, 23], which is related to both the microvasculature geometrical abnormalities and a reduction of the interstitial space [15]. As a result, the pressure gap across the capillary wall is small, hence the effectiveness of anti-cancer therapies can be compromised because of disordered blood flow in the vessels and a reduced distribution of drug molecules reaching the tumor cells through advection. To improve anti-cancer strategies and make their effects more predictable, understanding the relationship between the physical phenomena underlying the drug delivery process and the tumor system properties is essential.

Several mathematical models have been proposed in the last decade to investigate the microscopic inhomogeneity of tumors, that are composed by proliferating, apoptotic, healthy cells end extracellular matrix. The mixture theory has been exploited in the general context of fluid flow through porous media to derive the well-known models that rely, for example, on Darcy's and Brinkman's equations [41] and, more specifically, to address both the avascular and the vascular stages of tumor growth, stating and solving numerically the equations of mass, momentum and energy balance for several species [37, 1, 45, 46]. Following this approach, the macroscale equations are not obtained using upscaling arguments from microstructural balance, but they are *a priori* stated, or at most obtained on the basis of pure averaging. The governing equations and the constitutive equations then mimick the behavior that single components have *in bulk* and the interaction forces between components are deduced from heuristic arguments. Mixture theory models can be quite general, including any number of interacting species, nonlinear behavior and no apparent restriction on the geometrical features of the microstructure [32]. A substantial effort has been made to derive homogenized solutions and proper error estimates for a wide range of multiscale physical problems, in order to both encode the relevant microstructural information and improve computational cost (see, e.g. [55, 33, 43] for multi-phase composite materials and molecular dynamics).

In this paper we address the tumor microcirculation by an approach that also aims to account for the gross behavior of the system in terms of averaged equations. However, the multiple scale (*homogenization*) technique is able to upscale the

parameters of the macro equations on the basis of microstructural arguments. The multiple-scales method [44, 17] has been successfully applied to various physical systems, a most important field of applications of this technique being porous media flow (see e.g.[2]); rigorous homogenization has been successfully applied to the interaction between flow, chemical reactions and mechanics in cell tissues [18, 19], and also to deduce effective transmission condtions for reaction-diffusion processes in domain separated by an interface [31]. The use of this technique in investigating living systems is recent; a remarkable example of multiscale analysis applied to the fluid and drug transport in the microvasculature can be found in [49]. There, the derivation is obtained by scaling the various physical numbers (which arise from a proper non-dimensionalization of the microscale model) according to their order of magnitude, based on several examples which can be found in the biophysical literature. Furthermore, the blood is assumed to behave as a Newtonian fluid in a locally periodic and macroscopically uniform domain: macroscopic variations of the relevant fields are allowed, but macroscale variations of the microstructure, which might be relevant in malignant vascular networks, are not. Here, we follow a slightly different approach and derive a macroscale model which generalizes that in [49]; the latter can be recovered under a number of simplifying assumptions.

More specifically, we develop a mathematical model which describes the fluid and drug transport phenomena on the tissue length scale, accounting for both the crucial role of the tumor vasculature geometry and the mutual influence of mass and fluid transcapillary exchange. In our work, we are able to deal with general interface conditions at the boundary between vessels and tumor interstitium. In particular, we adopt a non-equilibrium (possibly non-linear) thermodynamic approach [26] to track the influence of the concentration of drug molecules on the fluid flow (i.e the osmotic pressure) and to account for the convection of drug across the capillary walls. We enforce the sharp length scale separation between the intercapillary distance and the tumor size, then we state the differential model on the physical domain. Here, non-dimensionalization and scaling are performed accounting for the physical behavior of the representative quantities with respect to the asymptotic expansion parameter (the ratio between the intercapillary distance and the characteristic tissue scale), rather than their order of magnitude, which might depend strongly on the specific biophysical system at hand. This approach allows us to describe the greatest possible number of physical phenomena at leading order, though an order of magnitude estimate of the relevant non-dimensional numbers can be *a posteriori* performed to evaluate the relative importance of the various parameters. Further, our results account for possible macroscopic variations of the microstructure and for changes in the effective viscosity due to possible spatial heterogeneities.

The final macroscale model for the physical quantities of interest, such as velocity, concentration and pressure field, describe the blood dynamics through a double Darcy's system of differential equations, whereas the drug dynamics is represented by a double advection-diffusion-reaction system. The interstitial and capillary models are coupled through effective mass sources which account for the fluid and drug

transport interplay. The present mathematical model is computationally feasible, because the key role of the microvascular geometry is encoded in the effective parameters of the macroscale model, which can be computed solving standard differential problems on a single cell. Hence, in perspective, numerical results obtained from such a model might help to predict the effectiveness of anti-cancer therapies.

The paper is organized as follows:

- Section 2 is devoted to formulate the continuum mechanics balance equations and the corresponding boundary conditions on the physical domain characterized by the intercapillary distance length scale, so that the distinction between the interstitial and capillary compartment is pointed out.
- In section 3 the governing equations are rewritten in non-dimensional form.
- In section 4 we apply a two-scales asymptotic expansion to obtain the effective governing equations describing the physical behaviour of the system on the tissue scale. The main result is summarized and discussed in 4.3. The fluid dynamics is modeled via a double Darcy's differential system, whereas the drug dynamics is represented by a double advection-diffusion-reaction model. The model reported in [49] is recovered as a special case.
- In section 5 some concluding remarks and future perspective are drawn.

2. Balance equations

In this paper we formulate a mathematical model for fluid and drug transport in a biological tissue permeated by a capillary network on the basis of a two-scale asymptotic expansion. The domain $\Omega \subset \mathbb{R}^3$ is composed of two subdomains, Ω_n and Ω_t, the capillary network and the tissue interstitium, respectively. Following the available biological literature, we assume the typical mean intercapillary distance d to be small compared to the tissue characteristic length L, so that we define a suitable spatial scale ratio as

$$\epsilon = \frac{d}{L} \ll 1. \tag{2.1}$$

According to the analysis reported in [27], the mean intercapillary distance is about $50\,\mu m\,(d \approx 10^{-5}\,\mathrm{m})$, whereas, for a tumor, the characteristic length can vary between $1\,\mathrm{cm}$ and $12\,\mathrm{cm}$ [51]; hence $L \approx 10^{-2} - 10^{-1}\,\mathrm{m}$ and

$$\epsilon \approx 10^{-4} - 10^{-3}. \tag{2.2}$$

At this stage, every unknown field of interest, such as the pressure p, the concentration of drug c and the blood velocity $\boldsymbol{u}$, is in principle a function of space $\boldsymbol{x}$ and time t. These quantities obey to balance laws that take specific form depending on the portion of the domain of interest and, in general, they are not continuous across subdomains interface. In particular, their restrictions to the interstitial and capillary compartment are denoted by subscripts t and n, respectively. We first consider the fluid and drug transport in each portion of Ω, then we will provide the proper interface conditions in order to close the resulting coupled differential problem.

2.1. *Interstitial Fluid flow*

The tumor interstitium Ω_t is here considered to be a non-deformable, isotropic porous medium, where the intracellular space represents the pores and Darcy's law applies:

$$\boldsymbol{u}_t = -\kappa\nabla p_t \quad \text{in } \Omega_t \tag{2.3}$$

$$\nabla \cdot \boldsymbol{u}_t = 0 \quad \text{in } \Omega_t, \tag{2.4}$$

where κ denotes the tissue hydraulic conductivity, which, in tumors, may vary dramatically depending on the tissue type and its chemical composition [52].

We assumed the medium isotropy for the sake of simplicity only. This assumption could be easily relaxed when replacing κ with a second order positive definite symmetric tensor to account for anisotropy, with some more complicated notations, but no increased insight from a physical viewpoint.

2.2. *Capillary fluid flow*

Blood is a non-Newtonian fluid, composed by the plasma (which can be regarded as a Newtonian solution made of water and proteins) and red blood cells, at a concentration (haematocrit) of $40 - 45\%$. A detailed analysis of blood rheology, regarding in particular its shear thinning behavior (i.e the apparent viscosity decreases with increasing shear rate), can be found for example in [13]. In particular, in vessels much larger than red blood cells (i.e $\approx 4\mu m$ [24]), at constant temperature and haematocrit, blood can be assumed to behave (approximately) as a Newonian fluid, with viscosity greater than plasma.
In small capillaries, a more complex blood rheology should be taken into account, since non-Newtonian effects, such as the Fahareus effect, the Fahareus-Lindqvist effect [12] and phase separation at bifurcations occur [38]. The typical diameter of the capillaries is comparable with the size of red blood cells, both in healthy (from 5 to $8\mu m$, [50]) and malignant tissues (values ranging from 10 to $30\mu m$ are reported, for example, in [21]).
Without entering delicate theoretical questions about possible constitutive relations for blood flow at such scales, here we consider it as a viscous fluid where the effective viscosity explicitly depends on the radius of the vessel r. In other words, we tacitly enforce a complex rheology of the blood, adopting an effective viscosity that depends on the radius, where such a spatial dependence is the *result* of an immaterial non-Newtonian constitutive law applied to a specific geometry.
For example, according to [39] and [36], when haematocrit and temperature are fixed to 45% and $37°C$, respectively, the flow in a straight vessel can be recovered by adopting an effective viscosity μ_e given by:

$$\mu_e = \mu \left(220\exp(-2.6r) + 3.2 - 2.44\exp(-0.06(2r)^{0.645})\right), \tag{2.5}$$

where $\mu \approx 1.16 - 1.33 \cdot 10^{-3}\,\mathrm{Pa\,s}$ [9] denotes plasma viscosity. Whenever the capillary network is regular enough that an average representative radius can be identified,

6   *R. Penta D.Ambrosi A. Quarteroni*

the viscosity can be considered constant, such that its value can be computed by means of (2.5). For example, for $r = 10\mu m$, we obtain $\mu_e = 1.59\mu$, whereas the the blood viscosity in large vessels, which is $\approx 4 \cdot 10^{-3}\,\mathrm{Pa\,s}$ [42], is reached only when r is approaching $200\mu m$, such that $\mu_e \approx 3.2\mu \approx 4 \cdot 10^{-3}\,\mathrm{Pa\,s}$.

Since the angiogenic capillary network embedded in a tumor mass typically exhibits strong spatial eterogeneities, we account for possible spatial variations in the (effective) capillary diameter. This can be performed, for example, replacing r in (2.5), with a suitable function $r = r(\boldsymbol{x})$, yielding

$$\mu_e = \mu_e(\boldsymbol{x}); \tag{2.6}$$

r is in principle a function of $\boldsymbol{x}$ depending on the geometric characteristics of the capillary network at hand (this can also be induced by medical images inspection). Finally, inertial and body forces can be ignored and the blood capillary flow is governed by the following Stokes' problem:

$$\mu_e \nabla^2 \boldsymbol{u}_n = \nabla p_n \quad \text{in } \Omega_n \tag{2.7}$$

$$\nabla \cdot \boldsymbol{u}_n = 0 \quad \text{in } \Omega_n. \tag{2.8}$$

2.3. *Drug transport, reaction and diffusion*

The combined action of transport and diffusion determines the concentration of drug in the blood vessels, whereas, in a tumor, cellular uptake ("the reaction") plays a major role. We thus assume a standard advection-diffusion equation for the concentration in the capillaries c_n, whereas an advection-diffusion-reaction equation holds for the concentration c_t in the tissue interstitium:

$$\frac{\partial c_n}{\partial t} + \nabla \cdot (c_n \boldsymbol{u}_n - D_n \nabla c_n) = 0 \quad \text{in } \Omega_n \tag{2.9}$$

$$\frac{\partial c_t}{\partial t} + \nabla \cdot (c_t \boldsymbol{u}_t - D_t \nabla c_t) = -h(c_t) \quad \text{in } \Omega_t. \tag{2.10}$$

Here D_n and D_t are the species diffusivity in their own subdomains and $h(c_t)$ is a positive, possibly non-linear function of the interstitial concentration, which accounts for the reaction mechanisms occurring in the system. When linear uptake only is relevant, we can prescribe:

$$h(c_t) = \gamma c_t, \tag{2.11}$$

where γ is the reaction uptake rate.

2.4. *Physiological interface fluxes*

The fluxes across the capillary wall can be obtained on the basis of non-equilibrium thermodynamic arguments, originally developed in [26] and then generalized to

other bio-physical systems [11, 54]. When assuming that the Kedem-Katchalsky formulation applies for both blood and drug fluxes, we obtain

$$\phi_b = L_p\left[(p_n - p_t) - \sigma RT(c_n - c_t)\right] \qquad (2.12)$$

$$\phi_d = \phi_b(1 - \sigma)c_m + P(c_n - c_t). \qquad (2.13)$$

where ϕ_b and ϕ_d denote the blood and drug fluxes per unit of total exchange surface area, respectively, whereas L_p is the hydraulic conductivity of the vessel wall, which accounts for the fluid leakage from the capillaries. In tumors, it can be up to two orders of magnitude higher than in healthy tissue, because of the openings and defects that characterize the tumor blood vascular networks [23]. Here, R is the universal gas constant, T is the absolute temperature, P is the diffusive permeability of the vessel wall. The osmotic reflection coefficient $(0 < \sigma < 1)$ quantifies the departure of a membrane behavior from semipermeability. For an ideal semipermeable membrane (no solute flux due to convection) $\sigma = 1$, so that the osmotic flow is maximized, whereas for an unselective membrane there is no osmosis and hence $\sigma = 0$. The value of σ depends on the relative geometry and size of the specific molecule and of the membrane pores [4].

According to (2.12), the blood flux across the interface is due both to the hydrostatic pressure drop and the osmotic pressure difference, the latter being proportional to the concentration jump for dilute solutions. The drug flux in (2.13) is the sum of a convective term, proportional to the fluid flux, and a diffusive one, proportional to the difference in concentration. The term c_m has the dimension of a concentration; in [54] it is suggested that it is a non-linear function of the fluid flux ϕ_b of the type:

$$c_m = (1 - f)c_n + fc_t; \quad f := \frac{1}{\tilde{\lambda}\phi_b} - \frac{1}{\exp(\tilde{\lambda}\phi_b) - 1} \quad \tilde{\lambda} := \frac{1 - \sigma}{P}. \qquad (2.14)$$

The quantity $\tilde{\lambda}\phi_b$ (at fixed blood flux ϕ_b) is often called the *transvascular* Péclet number (Pe$_v$), as it expresses the relative importance of convection to diffusion across the capillary walls. It is worth recalling the linearized analogues of relationship (2.13) when extreme values of Pe$_v$ are taken into account, namely:

$$\phi_d = \phi_b(1 - \sigma)c_n + P(c_n - c_t) \quad \text{for Pe}_v \gg 1 \qquad (2.15)$$

and

$$\phi_d = \phi_b(1 - \sigma)\bar{c} + P(c_n - c_t) \; ; \; \bar{c} = \frac{c_n + c_t}{2} \quad \text{for Pe}_v \ll 1. \qquad (2.16)$$

The relationship (2.13) is widely accepted in the bio-physical literature (see for example [22, 53]), whereas the approximation (2.16) has been previously adopted, for example, in [11]. A rough approximation for the drug flux, which rigorously applies only when the blood flux ϕ_b is negligible [20], yields a membrane law of the type:

$$\phi_d = P(c_n - c_t), \qquad (2.17)$$

which has been proposed in [28, 29].

Remark 2.1. According to the most widely accepted bio-physical literature [see for example 22], equation (2.12) should read:

$$\phi_b = L_p\left[(p_n - p_t) - \sigma(\pi_n - \pi_t)\right], \tag{2.18}$$

where $(\pi_n - \pi_t)$ denotes the osmotic pressure difference due to different concentrations of plasma proteins across the vessel walls. However, the present work is mostly related to malignant tissue, so that, according to the analysis reported in [23], the typical capillary pore dimensions ($\approx \mu m$) are much larger than the hydrodynamic radius of plasma proteins (for example, the typical radius of albumin is $\approx 3.5\ nm$). As a result, the osmotic pressure contribution due to plasma proteins is negligible in tumors. It is worth remarking that this could not be the case, in general, for drug macromolecules, whose radius can reach dramatically higher values with respect to plasma proteins (for example, particles characterized by a radius of $\approx 100-150\ nm$, have been recently developed [47]). We then argue that, in tumors, even though the blood flux is mostly driven by the pressure drop, the most general flux prescription is of the type (2.12), whereas, in healthy tissues, an accurate blood flux prescription should account for the osmotic pressure contribution, as in (2.18).

2.5. *Interface conditions*

We assume continuity of the drug and blood fluxes through the interface boundary $\Gamma = \partial\Omega_n \cap \partial\Omega_t$ via the following interface conditions:

$$\boldsymbol{u}_n \cdot \boldsymbol{n} = \boldsymbol{u}_t \cdot \boldsymbol{n} = \tilde{\phi}_b \tag{2.19}$$

$$(c_n\boldsymbol{u}_n - D_n\nabla c_n) \cdot \boldsymbol{n} = (c_t\boldsymbol{u}_t - D_t\nabla c_t) \cdot \boldsymbol{n} = \tilde{\phi}_d, \tag{2.20}$$

where $\boldsymbol{n}$ is the outward unit vector normal to the capillary surface, whereas we denote by

$$\tilde{\phi}_b = \phi_b(\hat{p}_n, p_t, c_n, c_t), \tag{2.21}$$

$$\tilde{\phi}_d = \phi_d(\hat{p}_n, p_t, c_n, c_t) \tag{2.22}$$

the fluxes prescriptions (given, in their general form, by (2.12, 2.13)) as functions of the normal component of the viscous stress, rather than the sole pressure, namely:

$$\hat{p}_n = p_n - \mu_e[(\boldsymbol{n} \cdot \nabla)\boldsymbol{u}_n] \cdot \boldsymbol{n}. \tag{2.23}$$

Remark 2.2. Although the viscous term in (2.23) is usually neglected in the physiological blood flux formulations, replacing p_n with $\hat{p}_n$ in (2.12) does not change its physical meaning, as it reads, in any case, proportional to the relevant normal mechanical stresses difference across the vessels membrane. Further, it is well known

that boundary conditions involving the Stokes' pressure should include the viscous contribution as well, as this is necessary to get a coherent variational form of the problem, which can in turn lead model well-posedness (see, e.g. [10]) and convenient *a priori* estimates for justifying the convergence of the homogenization process (as in [2]).

Remark 2.3. According to the biophysical literature (see, e.g. [22, 23]), the actually measured physical quantities are the average macroscopic blood and drug fluxes. For example the blood flux, which is often referred to as J_v, reads:

$$J_v = S\phi_b, \tag{2.24}$$

where S is the total exchange surface of the capillary vessels and ϕ_b is given by (2.12) or (2.18) depending on the actual physical system at hand. Even though it is more convenient to prescribe the fluxes per unit area in the current formulation, we still have to account for the correct asymptotic behavior of the various physical quantities involved in the extravasation process. In fact, it is reasonable to assume that the actual measured flux (i.e of the type (2.24)) for a fixed portion of the tissue is finite, even when the number of capillaries (and correspondingly their total surface) increases within the volume, so that the average distance between them decreases, that is:

$$S \propto N \propto \frac{L}{d} = \frac{1}{\epsilon} \rightarrow \phi_b \propto \frac{1}{N} \propto \frac{d}{L} = \epsilon, \tag{2.25}$$

where N is the (estimated) average capillary number in the network. We apply the heuristic argument (2.25) highlighting the correct asymptotic behavior of both the blood and drug fluxes per unit area, $\tilde{\phi}_b$ and $\tilde{\phi}_d$, via the following definitions:

$$\tilde{\phi}_b = \epsilon\Phi_b, \quad \tilde{\phi}_d = \epsilon\Phi_d, \tag{2.26}$$

and for the sake of simplicity, from now on, we still refer to the quantities Φ_b and Φ_d as the blood and drug flux, respectively. The interface conditions (2.19-2.20) then rewrite:

$$\boldsymbol{u}_n \cdot \boldsymbol{n} = \boldsymbol{u}_t \cdot \boldsymbol{n} = \epsilon\Phi_b \tag{2.27}$$

$$(c_n\boldsymbol{u}_n - D_n\nabla c_n) \cdot \boldsymbol{n} = (c_t\boldsymbol{u}_t - D_t\nabla c_t) \cdot \boldsymbol{n} = \epsilon\Phi_d. \tag{2.28}$$

The ϵ coefficient appearing on the right hand sides of (2.27-2.28) then reflects the application of average experimental measures to a local balance law. In fact, this is the proper scaling to ensure that local fluxes contributions, which are expected to translate into volumetric contribution on the global scale, are finite in the limit for $\epsilon \rightarrow 0$.

To close the problem, we need one more boundary condition for the tangent components of the fluid velocity in the capillaries. Since the solid compartment is a porous medium, following [25], we assume that the following generalized slip conditions [3] hold

$$\boldsymbol{u_n} \cdot \boldsymbol{\tau} = -\frac{\sqrt{k}}{\alpha}\left[(\boldsymbol{n} \cdot \nabla)\boldsymbol{u_n}\right] \cdot \boldsymbol{\tau} \text{ on } \Gamma, \tag{2.29}$$

where α is a non-dimensional parameter, which depends on the properties of the porous surface, $\boldsymbol{\tau}$ is any unit vector tangent to the capillary surface and k is the tissue permeability, which is related to the hydraulic conductivity κ by

$$\kappa = \frac{k}{\mu_e}. \tag{2.30}$$

3. Non-dimensional form of the equations

Equations (2.3), (2.4), (2.7), (2.8), (2.9), (2.10), equipped with boundary conditions (2.27), (2.28), (2.29) and proper effective viscosity and fluxes prescriptions (for example of the type (2.5,2.6) and (2.12,2.13), respectively), represent a coupled system of partial differential equations in the variables $\boldsymbol{u}_n$, $\boldsymbol{u}_t$, p_n, p_t, c_n, c_t on the whole domain Ω, which includes both the tumor interstitium Ω_t and the capillary network Ω_n. We now rewrite the system in non-dimensional variables:

$$\boldsymbol{x} = L\boldsymbol{x'} \quad \boldsymbol{u} = \frac{Cd^2}{\mu}\boldsymbol{u'} \quad p = CLp' \quad c = C_r c' \quad t = \frac{L\mu}{Cd^2}t', \tag{3.1}$$

where C_r, C are the reference concentration and pressure gradient, respectively. The corresponding system of partial differential equations in non-dimensional form then reads (the primes have been dropped for the sake of simplicity):

$$\bar{\mu}\epsilon^2\nabla^2\boldsymbol{u}_n = \nabla p_n \quad \text{in } \Omega_n \tag{3.2}$$

$$\nabla \cdot \boldsymbol{u}_n = 0 \quad \text{in } \Omega_n \tag{3.3}$$

$$\boldsymbol{u}_t = -\bar{\kappa}\nabla p_t \quad \text{in } \Omega_t \tag{3.4}$$

$$\nabla \cdot \boldsymbol{u}_t = 0 \quad \text{in } \Omega_t \tag{3.5}$$

$$\frac{\partial c_n}{\partial t} + \nabla \cdot (c_n\boldsymbol{u}_n - A_n\nabla c_n) = 0 \quad \text{in } \Omega_n \tag{3.6}$$

$$\frac{\partial c_t}{\partial t} + \nabla \cdot (c_t\boldsymbol{u}_t - A_t\nabla c_t) = -\bar{h}(c_t) \quad \text{in } \Omega_t \tag{3.7}$$

supplemented by the interface conditions

$$\boldsymbol{u}_n \cdot \boldsymbol{n} = \epsilon\bar{\Phi}_b \quad \text{on } \Gamma \tag{3.8}$$

$$\boldsymbol{u}_n \cdot \boldsymbol{\tau} = -\epsilon\phi\left[(\boldsymbol{n} \cdot \nabla)\boldsymbol{u_n}\right] \cdot \boldsymbol{\tau} \quad \text{on } \Gamma \tag{3.9}$$

$$\boldsymbol{u}_t \cdot \boldsymbol{n} = \epsilon\bar{\Phi}_b \quad \text{on } \Gamma \tag{3.10}$$

$$(c_n\boldsymbol{u}_n - A_n\nabla c_n) \cdot \boldsymbol{n} = \epsilon\bar{\Phi}_d \quad \text{on } \Gamma \tag{3.11}$$

$$(c_t\boldsymbol{u}_t - A_t\nabla c_t) \cdot \boldsymbol{n} = \epsilon\bar{\Phi}_d \quad \text{on } \Gamma, \tag{3.12}$$

where $\bar{\Phi}_b$, $\bar{\Phi}_d$, $\bar{h}$ are the corresponding non-dimensional blood and drug fluxes and reaction function, respectively. Whenever the most general Kedem and Katchalsky formulation of the type (2.12-2.13) is adopted, the resulting non-dimensional fluxes read:

$$\bar{\Phi}_b = \bar{L}_p \left(\hat{p}_n - p_t \right) - \bar{\Pi} \left(c_n - c_t \right), \tag{3.13}$$

$$\bar{\Phi}_d = \left(1 - \sigma \right) c_m \bar{\Phi}_b + \bar{\Upsilon} \left(c_n - c_t \right), \tag{3.14}$$

where $\hat{p}_n$ is the non-dimensional normal stress given by

$$\hat{p}_n = p_n - \epsilon^2 \bar{\mu}[(\boldsymbol{n} \cdot \nabla)\boldsymbol{u}_n] \cdot \boldsymbol{n}. \tag{3.15}$$

The non-dimensional numbers (functions) introduced above are defined as follows:

$$\bar{\mu}(\boldsymbol{x}) = \frac{\mu_e(\boldsymbol{x})}{\mu} \,;\, \bar{\kappa} = \frac{\kappa \mu}{d^2} \,;\, A_n = \frac{D_n \mu}{LCd^2} \,;\, A_t = \frac{D_t \mu}{LCd^2} \,;\, \phi = \frac{\sqrt{\kappa \bar{\mu}(\boldsymbol{x})}}{\alpha} \,;$$

$$\bar{L}_p = \frac{L_p L^2 \mu}{d^3} \,;\, \bar{\Pi} = \frac{L_p L \mu \sigma RTC_r}{Cd^3} \,;\, \bar{\Upsilon} = \frac{P\mu L}{Cd^3}. \tag{3.16}$$

Here, $\bar{\mu}$ represents the relative fluid viscosity, whereas $\bar{\kappa}$, ϕ are the non-dimensional hydraulic conductivity and slip coefficient, respectively. The number $\bar{L}_p$, $\bar{\Upsilon}$ are non-dimensional hydraulic vessels conductivity and diffusive permeability, whereas $\bar{\Pi}$ measures the relative importance of osmotic vs fluid pressure drop across the vessel wall. The non-dimensional numbers A_n and A_t express the relative importance of diffusion vs convection, so that they can be written as

$$A_n = \frac{1}{\text{Pe}_n}; \quad A_t = \frac{1}{\text{Pe}_t}, \tag{3.17}$$

where the capillary and interstitial Péclet numbers Pe_n and Pe_t are defined as

$$\text{Pe}_n := \frac{LCd^2}{D_n \mu}; \quad \text{Pe}_t := \frac{LCd^2}{D_t \mu}. \tag{3.18}$$

Further remarks about the choice (3.1) of non-dimensional variables and the meaning of the corresponding equations are in order.

The Stokes' type characteristic velocity

$$U = \frac{Cd^2}{\mu} \tag{3.19}$$

adopted in (3.1) preserves the asymptotic behavior of the interstitial fluid velocity, as well as in the capillaries (see continuity condition (2.27)) as $\epsilon \to 0$. Problem (3.2) is the typical asymptotic problem which characterizes the flow in porous media in the multiple scales analysis context, as, for example, in [7, 16, 2]. The transport parameters, including the tissue hydraulic conductivity and any other transvascular parameter encoded in the fluxes $\bar{\Phi}_b$, $\bar{\Phi}_d$ (for example, the membrane conductivity

L_p and the diffusive permeability P), are given by experimental measurements, that implicitly comprise a dependence on both the geometry and on the tissue and capillary walls material and chemical composition. Here, we claim that the observed Darcy's interstitial flow, together with the Kedem-Katchalsky leakage of blood and macromolecules from the vessels, should be consistent with the Stokes's type characteristic velocity profile assumed in (3.1). As a consequence, the non-dimensional tissue hydraulic conductivity given by (3.16) and the non-dimensional fluxes are to be considered fixed in the limit $\epsilon \to 0$. Finally, we assume a formal balance between diffusion, reaction and convection within the domain, so that the Péclet numbers (3.18) and the non-dimensional reaction $\bar{h}$ are fixed in the limit $\epsilon \to 0$. This is done for the sake of generality, as this approach allows us to retain the greatest possible number of physical phenomena in the asymptotic analysis. However, the relative importance of the various phenomena can be *a posteriori* evaluated via an order of magnitude estimate of the resulting non-dimensional numbers, to account for specific physical regimes (such as, for example, the advection dominated regime), depending on the actual physical system at hand.

4. Multiscale formulation

In this section we employ the two-scales technique [44, 17] to derive a continuum macroscale model for the system of equations (3.2-3.12). Since $\epsilon \ll 1$, we enforce the sharp length scale separation between the intercapillary distance d, the *microscale*, and the tissue characteristic dimension L, the *macroscale*, (see figure 1) defining:

$$\boldsymbol{y} := \frac{\boldsymbol{x}}{\epsilon}. \tag{4.1}$$

Following the usual approach in multiscale analysis, from now on $\boldsymbol{x}$ and $\boldsymbol{y}$ denote independent variables, representing the macro and micro spatial scale, respectively. We then assume that any unknown field ψ defined throughout this work (i.e. $\boldsymbol{u}_n$, $\boldsymbol{u}_t$, p_n, p_t, c_n, c_t) is a function of these independent spatial variables:

$$\psi = \psi(\boldsymbol{x}, \boldsymbol{y}, t)$$

so that the differential operators transform accordingly:

$$\nabla \to \nabla_{\boldsymbol{x}} + \frac{1}{\epsilon}\nabla_{\boldsymbol{y}}; \quad \nabla^2 \to \frac{1}{\epsilon^2}\nabla_{\boldsymbol{y}} + \frac{2}{\epsilon}\nabla_{\boldsymbol{y}} \cdot \nabla_{\boldsymbol{x}} + \nabla_{\boldsymbol{x}}^2. \tag{4.2}$$

For every field ψ we formally perform the following multiple scales expansion in power series of ϵ:

$$\psi = \psi_{\epsilon}(\boldsymbol{x}, \boldsymbol{y}, t) = \sum_{l=0}^{\infty} \psi^{(l)}(\boldsymbol{x}, \boldsymbol{y}, t)\epsilon^l. \tag{4.3}$$

The components $\psi^{(l)}$ are defined for every $\boldsymbol{x}$ belonging to the macroscale domain, whereas $\boldsymbol{y}$ spans only the specific portion of the microscale where ψ is defined. We assume periodicity in the microscale variable, so that every $\psi^{(l)}$ is $\boldsymbol{y}$-periodic.
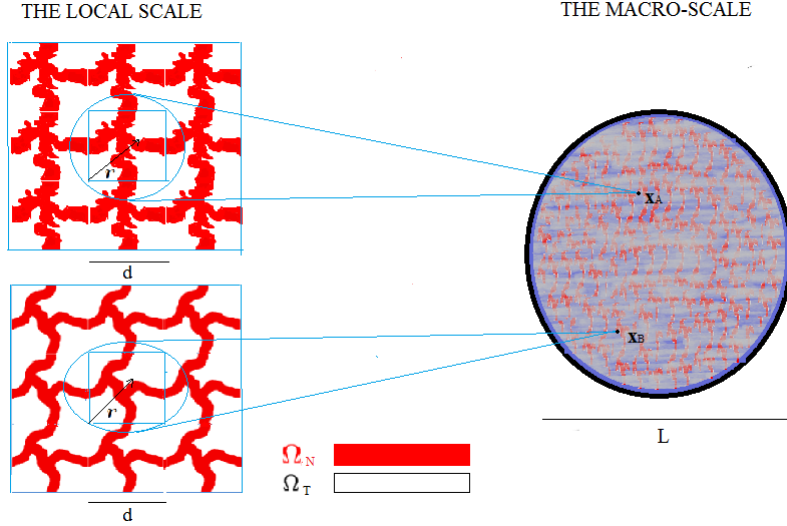
Fig. 1. A 2D cartoon representing the micro and macro scales. On the right hand side, the homogenized domain, where the microstructure is smoothed out, is shown. On the left hand side, the microscale is shown and the difference between the interstitial and capillary compartment is pointed out. Two possible examples of periodic units (drawn as blue circles) are depicted, related to two different macroscale points denoted by $\boldsymbol{x}_A$ and $\boldsymbol{x}_B$, to emphasize that the medium is not, in general, macroscopically uniform. In fact, the interface position vector $\boldsymbol{r}$ related to the same (homologous by $\boldsymbol{y}$-periodicity) local point is varying with respect to $\boldsymbol{x}$, that is $\boldsymbol{r}(\boldsymbol{x}_A, \boldsymbol{y}) \neq \boldsymbol{r}(\boldsymbol{x}_B, \boldsymbol{y})$. Whenever the medium exhibits such variations, one cell problem for every $\boldsymbol{x}$ of the homogenized domain is to be solved.

Remark 4.1. Only *local* periodicity is assumed, while macroscale variation in any field ψ is allowed. Furthermore, the interstitial and capillary compartments can also macroscopically vary, that is $\Omega_n = \Omega_n(\boldsymbol{x}, \boldsymbol{y})$, $\Omega_t = \Omega_t(\boldsymbol{x}, \boldsymbol{y})$, so that possible macroscale changes of geometry are accounted for. This represents a difference with respect to previous works [2, 49], where the medium is assumed *macroscopically uniform*, i.e. the interface between subdomains is assumed to be $\boldsymbol{x}$-constant, so that the geometric structure of the medium is globally periodic, even though macroscopic variations of the fields are obviously still allowed. Note that the latter assumption is much stronger than local periodicity only, especially for tumor vascular networks, which exhibit sharp spatial heterogeneities.

We perform power series expansions of the form (4.3) for the relevant fields in (3.2-3.12); by collecting coefficients of ϵ^l for $l = 0, 1, ...$, and exploiting suitable microscale averages, we derive a closed macroscale model for the leading order fields $p_n^{(0)}$, $p_t^{(0)}$, $c_n^{(0)}$, $c_t^{(0)}$, $\boldsymbol{u}_n^{(0)}$, $\boldsymbol{u}_t^{(0)}$.

Whenever a component of the asymptotic expansion retains a dependence on the

14   *R. Penta D.Ambrosi A. Quarteroni*

microscale $\boldsymbol{y}$, we can take its integral average, defined as follows:

$$\langle\psi\rangle_s = \frac{1}{|\Omega_s|}\int_{\Omega_s}\psi(\boldsymbol{x},\boldsymbol{y},t)\,\mathrm{d}\boldsymbol{y}, \quad s = t,n \tag{4.4}$$

where $|\Omega_t|$ and $|\Omega_n|$ stand for the interstitial and capillary volume, respectively, and integration is performed over the local scale $\boldsymbol{y}$. Because of the $\boldsymbol{y}$-periodicity, the integral average (4.4) does not change if performed over a single representative cell only (that is, when Ω_s is replaced by its representative cell portion), so that, from now on, (4.4) will be regarded as a cell average. Finally, we also permit macroscale variations of the capillary radius r, such that from now on we assume:

$$\bar{\mu} = \bar{\mu}(\boldsymbol{x}), \tag{4.5}$$

that is, $\bar{\mu}$ is $\boldsymbol{y}$-constant.

4.1. *Capillary problem*

Assuming that all the fields depend on the independent variables $(\boldsymbol{x}, \boldsymbol{y})$, derivatives transform according to (4.2), so that the capillary problem in Ω_n (3.2-3.3), (3.6), (3.8-3.9), (3.11), rewrites:

$$\bar{\mu}\epsilon\nabla_{\boldsymbol{y}}^2\boldsymbol{u}_n + 2\bar{\mu}\epsilon^2\nabla_{\boldsymbol{y}}\cdot\nabla_{\boldsymbol{x}}\boldsymbol{u}_n + \bar{\mu}\epsilon^3\nabla_{\boldsymbol{x}}^2\boldsymbol{u}_n = \nabla_{\boldsymbol{y}}p_n + \epsilon\nabla_{\boldsymbol{x}}p_n \tag{4.6}$$

$$\nabla_{\boldsymbol{y}}\cdot\boldsymbol{u}_n + \epsilon\nabla_{\boldsymbol{x}}\cdot\boldsymbol{u}_n = 0 \tag{4.7}$$

$$\epsilon^2\frac{\partial c_n}{\partial t} + \nabla_{\boldsymbol{x}}\cdot\left(\epsilon^2 c_n\boldsymbol{u}_n - \epsilon A_n\nabla_{\boldsymbol{y}}c_n - \epsilon^2 A_n\nabla_{\boldsymbol{x}}c_n\right)$$
$$+\nabla_{\boldsymbol{y}}\cdot\left(\epsilon c_n\boldsymbol{u}_n - A_n\nabla_{\boldsymbol{y}}c_n - \epsilon A_n\nabla_{\boldsymbol{x}}c_n\right) = 0 \tag{4.8}$$

equipped with interface conditions on Γ of the form:

$$(\epsilon c_n\boldsymbol{u}_n - A_n\nabla_{\boldsymbol{y}}c_n - \epsilon A_n\nabla_{\boldsymbol{x}}c_n)\cdot\boldsymbol{n} = \epsilon^2\bar{\Phi}_d \text{ on } \Gamma \tag{4.9}$$

$$\boldsymbol{u}_n\cdot\boldsymbol{n} = \epsilon\bar{\Phi}_b \tag{4.10}$$

$$-\phi\left[(\boldsymbol{n}\cdot\nabla_{\boldsymbol{y}})\boldsymbol{u}_n\right]\cdot\boldsymbol{\tau} - \epsilon\phi\left[(\boldsymbol{n}\cdot\nabla_{\boldsymbol{x}})\boldsymbol{u}_n\right]\cdot\boldsymbol{\tau} = \boldsymbol{u}_n\cdot\boldsymbol{\tau} \text{ on } \Gamma, \tag{4.11}$$

where, enforcing (4.2), the general formulation for the fluid and drug non-dimensional fluxes (3.13,3.14) reads:

$$\bar{\Phi}_b = \bar{L}_p\left(p_n - p_t\right) - \bar{\Pi}\left(c_n - c_t\right) - \bar{L}_p\epsilon\bar{\mu}[(\boldsymbol{n}\cdot\nabla_{\boldsymbol{y}})\boldsymbol{u}_n]\cdot\boldsymbol{n} - \bar{L}_p\epsilon^2\bar{\mu}[(\boldsymbol{n}\cdot\nabla_{\boldsymbol{x}})\boldsymbol{u}_n]\cdot\boldsymbol{n}, \tag{4.12}$$

$$\bar{\Phi}_d = (1-\sigma)\,c_m\bar{\Phi}_b + \bar{\Upsilon}\left(c_n - c_t\right). \tag{4.13}$$

Our aim is to determine a closed problem for the zero-th order fields $p_n^{(0)}$, $\left\langle\boldsymbol{u}_n^{(0)}\right\rangle_n$, $c_n^{(0)}$. We start considering the fluid flow in the capillaries; collecting terms of order ϵ^0 in (4.6) we get

$$\nabla_{\boldsymbol{y}}p_n^{(0)} = 0 \rightarrow p_n^{(0)} = p_n^{(0)}(\boldsymbol{x},t). \tag{4.14}$$

Therefore, the leading order pressure field in the capillaries is $\boldsymbol{y}$-constant. Equating coefficients of ϵ^1 in (4.6) and ϵ^0 in (4.7), (4.10), (4.11), we obtain the following Stokes-type boundary value problem for $(\boldsymbol{u}_n^{(0)}, p_n^{(1)})$:

$$\nabla_{\boldsymbol{y}} p_n^{(1)} - \bar{\mu} \nabla_{\boldsymbol{y}}^2 \boldsymbol{u}_n^{(0)} = -\nabla_{\boldsymbol{x}} p_n^{(0)} \text{ in } \Omega_n \tag{4.15}$$

$$\nabla_{\boldsymbol{y}} \cdot \boldsymbol{u}_n^{(0)} = 0 \text{ in } \Omega_n \tag{4.16}$$

$$\boldsymbol{u}_n^{(0)} \cdot \boldsymbol{n} = 0 \text{ on } \Gamma \tag{4.17}$$

$$-\phi \left[(\boldsymbol{n} \cdot \nabla_{\boldsymbol{y}}) \boldsymbol{u}_n^{(0)} \right] \cdot \boldsymbol{\tau} = \boldsymbol{u}_n^{(0)} \cdot \boldsymbol{\tau} \text{ on } \Gamma \tag{4.18}$$

Now we exploit linearity of equations (4.15-4.18) together with (4.14) to formulate the following ansatz for the solution:

$$\boldsymbol{u}_n^{(0)}(\boldsymbol{x}, \boldsymbol{y}, t) = -\mathsf{W}(\boldsymbol{x}, \boldsymbol{y}) \nabla_{\boldsymbol{x}} p_n^{(0)}(\boldsymbol{x}, t) \tag{4.19}$$

$$p_n^{(1)}(\boldsymbol{x}, \boldsymbol{y}) = -\boldsymbol{P}_n(\boldsymbol{x}, \boldsymbol{y}) \cdot \nabla_{\boldsymbol{x}} p_n^{(0)}(\boldsymbol{x}, t) + \tilde{p}(\boldsymbol{x}, t), \tag{4.20}$$

where the cell fields $(\mathsf{W}, \boldsymbol{P}_n)$ satisy the following Stokes' type problem:

$$\nabla_{\boldsymbol{y}} \boldsymbol{P_n} = \bar{\mu} \nabla_{\boldsymbol{y}}^2 \mathsf{W}^{\mathsf{T}} + \mathsf{I} \quad \text{in } \Omega_n \tag{4.21}$$

$$\nabla_{\boldsymbol{y}} \cdot \mathsf{W}^{\mathsf{T}} = 0 \quad \text{in } \Omega_n \tag{4.22}$$

$$\mathsf{W}^{\mathsf{T}} \boldsymbol{n} = 0 \quad \text{on } \Gamma \tag{4.23}$$

$$-\phi [(\nabla_{\boldsymbol{y}} \mathsf{W}^{\mathsf{T}}) \boldsymbol{n}] \boldsymbol{\tau} = \mathsf{W}^{\mathsf{T}} \boldsymbol{\tau} \quad \text{on } \Gamma. \tag{4.24}$$

The above system of partial differential equations is supplemented by periodicity conditions in $\boldsymbol{y}$ together with suitable conditions that guarantee uniqueness for the auxiliary vector $\boldsymbol{P}_n$, for example:

$$\langle \boldsymbol{P}_n \rangle_n = 0. \tag{4.25}$$

We are now able to provide a macroscale equation for the average capillary velocity $\left\langle \boldsymbol{u}_n^{(0)} \right\rangle_n$. Integrating (4.19) over Ω_n we obtain:

$$\left\langle \boldsymbol{u}_n^{(0)} \right\rangle_n = -\mathsf{K} \nabla_{\boldsymbol{x}} p_n^{(0)} \tag{4.26}$$

where K is the second order permeability tensor for the capillary flow defined by:

$$\mathsf{K} = \langle W \rangle_n, \tag{4.27}$$

or, componentwise,

$$K_{ij} = \frac{1}{|\Omega_n|} \int_{\Omega_n} W_{ij} \, \mathrm{d} \boldsymbol{y} \quad i, j \in (1, 2, 3).$$

The average velocity profile in the capillaries thus obeys an anisotropic Darcy's law at the macroscale: the flow is driven by the leading order pressure in the capillaries $p_n^{(0)}$, whereas the microstructure is encoded in the permeability tensor K.

To obtain a macroscale equation for $p_n^{(0)}$, we collect the coefficients of order ϵ in (4.7):

$$\nabla_{\boldsymbol{x}} \cdot \boldsymbol{u}_n^{(0)} = -\nabla_{\boldsymbol{y}} \cdot \boldsymbol{u}_n^{(1)}, \tag{4.28}$$

hence

$$\left\langle \nabla_{\boldsymbol{x}} \cdot \boldsymbol{u}_n^{(0)} \right\rangle_n = -\left\langle \nabla_{\boldsymbol{y}} \cdot \boldsymbol{u}_n^{(1)} \right\rangle_n = -\frac{1}{|\Omega_n|} \int_{\Gamma} \boldsymbol{u}_n^{(1)} \cdot \boldsymbol{n} \, \mathrm{d}\mathrm{S}_y, \tag{4.29}$$

where we used the divergence theorem in $\boldsymbol{y}$ and exploited $\boldsymbol{y}$-periodicity. Further, the ϵ^1 contribution in the interface condition (4.10) yields:

$$\boldsymbol{u}_n^{(1)} \cdot \boldsymbol{n} = \bar{\Phi}_b^{(0)} \quad \text{on } \Gamma, \tag{4.30}$$

where we denote by $\bar{\Phi}_b^{(0)}$ the zero-th order non-dimensional blood flux, such that

$$\left\langle \nabla_{\boldsymbol{x}} \cdot \boldsymbol{u}_n^{(0)} \right\rangle_n = -\frac{1}{|\Omega_n|} \int_{\Gamma} \bar{\Phi}_b^{(0)} \, \mathrm{d}\mathrm{S}_y, \tag{4.31}$$

and, when a general presciption of the type (4.12) applies, $\bar{\Phi}_b^{(0)}$ is given by:

$$\bar{\Phi}_b = \bar{L}_p \left(p_n^{(0)} - p_t^{(0)} \right) - \bar{\Pi} \left(c_n^{(0)} - c_t^{(0)} \right). \tag{4.32}$$

In order to obtain a scalar equation for the leading order pressure $p_n^{(0)}$, it is convenient to exploit the previously derived linear relationship between the leading order capillary velocity and pressure (4.26). We first make use of the generalized Reynold's transport theorem [16] with respect to $\boldsymbol{x}$ to relate the cell average of the macroscale divergence of the leading order velocity field $\boldsymbol{u}_n^{(0)}$ to the divergence of its average (which are in principle different because $\Omega_n = \Omega_n(\boldsymbol{x}, \boldsymbol{y})$), that is:

$$\nabla_{\boldsymbol{x}} \cdot \left\langle \boldsymbol{u}_n^{(0)} \right\rangle_n = \left\langle \nabla_{\boldsymbol{x}} \cdot \boldsymbol{u}_n^{(0)} \right\rangle_n + \frac{1}{|\Omega_n|} \int_{\Gamma} \boldsymbol{u}_n^{(0)} \cdot \boldsymbol{q} \, \mathrm{d}\mathrm{S}_y, \tag{4.33}$$

where, according to preexisting literature examples in multiscale analysis (see, e.g. [7, 35]), we exploited the following notation:

$$\boldsymbol{q} := (\nabla_{\boldsymbol{x}} \boldsymbol{r}(\boldsymbol{x}, \boldsymbol{y}))^{\mathsf{T}} \boldsymbol{n}, \tag{4.34}$$

where $\boldsymbol{r}(\boldsymbol{x}, \boldsymbol{y})$ denotes the interface position vector [16] (see figure 1). Substituting equations (4.26) and (4.31) into (4.33) we finally obtain:

$$-\nabla_{\boldsymbol{x}} \cdot \left\langle \boldsymbol{u}_n^{(0)} \right\rangle_n = \nabla_{\boldsymbol{x}} \cdot \left(\mathsf{K} \nabla_{\boldsymbol{x}} p_n^{(0)} \right) = \frac{1}{|\Omega_n|} \int_{\Gamma} (\bar{\Phi}_b^{(0)} - \boldsymbol{u}_n^{(0)} \cdot \boldsymbol{q}) \, \mathrm{d}\mathrm{S}_y. \tag{4.35}$$

The fluid flow in the capillaries compartment is not incompressible at the macroscale. The effective source term appearing on the right hand side of (4.35) is firstly due to the leading order blood flux $\bar{\Phi}_b^{(0)}$. Hence, the microscale exchange between the interstitial and capillary compartment across the interface Γ translates into a volumetric contribution on the global length scale. The second term at the right hand side of (4.35) is the apparent flux due to possible variations of the microscale geometry with respect to the macroscale $\boldsymbol{x}$.

A macroscale equation for the leading order concentration in the capillaries is obtained collecting coefficients of ϵ^0 in (4.8), (4.9):

$$\nabla_{\boldsymbol{y}}^2 c_n^{(0)} = 0 \qquad \text{in } \Omega_n \tag{4.36}$$

$$\nabla_{\boldsymbol{y}} c_n^{(0)} \cdot \boldsymbol{n} = 0 \qquad \text{on } \Gamma. \tag{4.37}$$

This is a Laplace boundary value problem, with periodicity condition in $\boldsymbol{y}$ and homogeneous Neumann condition on Γ, whose solution

$$c_n^{(0)} = c_n^{(0)}(\boldsymbol{x}, t) \tag{4.38}$$

is constant with respect to $\boldsymbol{y}$. Collecting terms of order ϵ^1 in (4.8), (4.9) we obtain the following differential problem for $c_n^{(1)}$:

$$\nabla_{\boldsymbol{y}}^2 c_n^{(1)} = 0 \quad \text{in } \Omega_n \tag{4.39}$$

$$\nabla_{\boldsymbol{y}} c_n^{(1)} \cdot \boldsymbol{n} = -\nabla_{\boldsymbol{x}} c_n^{(0)} \cdot \boldsymbol{n} \quad \text{on } \Gamma, \tag{4.40}$$

where we accounted for the zero-th order incompressibility costraint (4.16) and for (4.38) to obtain equation (4.39), whereas (4.17) was exploited to get the interface condition (4.40). The solution of (4.39-4.40) is unique up to an arbitrary $\boldsymbol{y}$-constant function; as the leading order concentration $c_n^{(0)}$ is locally constant (4.38) and the problem is linear, we can state the following ansatz for the solution:

$$c_n^{(1)} = -\boldsymbol{a} \cdot \nabla_{\boldsymbol{x}} c_n^{(0)} + \bar{c}(\boldsymbol{x}, t), \tag{4.41}$$

where the auxiliary vector $\boldsymbol{a}(\boldsymbol{x}, \boldsymbol{y})$ solves the cell problem:

$$\nabla_{\boldsymbol{y}}^2 \boldsymbol{a} = 0 \quad \text{in } \Omega_n \tag{4.42}$$

$$(\nabla_{\boldsymbol{y}} \boldsymbol{a}) \boldsymbol{n} = \boldsymbol{n} \quad \text{on } \Gamma. \tag{4.43}$$

As previously, a further condition for $\boldsymbol{a}$ is required to ensure uniqueness, for example

$$\langle \boldsymbol{a} \rangle_n = 0. \tag{4.44}$$

Now we seek for a macroscale equation for the leading order concentration in the capillaries $c_n^{(0)}$. We start by equating ϵ^2 coefficients in (4.8),(4.9) to get:

$$\frac{\partial c_n^{(0)}}{\partial t} + \nabla_{\boldsymbol{x}} \cdot \left(c_n^{(0)} \boldsymbol{u}_n^{(0)} \right) - A_n \nabla_{\boldsymbol{x}} \cdot \left(\nabla_{\boldsymbol{y}} c_n^{(1)} \right) - A_n \nabla_{\boldsymbol{x}}^2 c_n^{(0)} + \nabla_{\boldsymbol{y}} \cdot \left(c_n^{(0)} \boldsymbol{u}_n^{(1)} \right)$$
$$+ \nabla_{\boldsymbol{y}} \cdot \left(c_n^{(1)} \boldsymbol{u}_n^{(0)} \right) - A_n \nabla_{\boldsymbol{y}}^2 c_n^{(2)} - A_n \nabla_{\boldsymbol{y}} \cdot \left(\nabla_{\boldsymbol{x}} c_n^{(1)} \right) = 0 \quad \text{in } \Omega_n, \tag{4.45}$$

$$\left(c_n^{(0)} \boldsymbol{u}_n^{(1)} + c_n^{(1)} \boldsymbol{u}^{(0)} - A_n \nabla_{\boldsymbol{y}} c_n^{(2)} - A_n \nabla_{\boldsymbol{x}} c_n^{(1)} \right) \cdot \boldsymbol{n} = \bar{\Phi}_d^{(0)} \quad \text{on } \Gamma, \tag{4.46}$$

where, when a general prescription of the type (4.13) applies, the zero-th order drug flux $\bar{\Phi}_d^{(0)}$ reads

$$\bar{\Phi}_d^{(0)} = (1 - \sigma) c_m^{(0)} \bar{\Phi}_b^{(0)} + \bar{\Upsilon} \left(c_n^{(0)} - c_t^{(0)} \right), \tag{4.47}$$

with $\bar{\Phi}_b^{(0)}$ given by (4.32). Integral average of (4.45) over Ω_n, when the divergence theorem together with $\boldsymbol{y}$-periodicity are enforced, yields:

$$\frac{\partial c_n^{(0)}}{\partial t} + \left\langle \nabla_{\boldsymbol{x}} \cdot \left(c_n^{(0)} \boldsymbol{u}_n^{(0)} \right) \right\rangle_n - A_n \nabla_{\boldsymbol{x}}^2 c_n^{(0)}$$
$$+ \frac{1}{|\Omega_n|} \int_{\Gamma} \bar{\Phi}_d^{(0)} \, \mathrm{dS}_y - A_n \left\langle \nabla_{\boldsymbol{x}} \cdot \left(\nabla_{\boldsymbol{y}} c_n^{(1)} \right) \right\rangle_n = 0. \tag{4.48}$$

The interface contributions have been evaluated by means of (4.46) and condition (4.38) has been explicitly exploited. The resulting macroscale equation (4.48) can be rewritten exploiting the Reynolds' transport theorem in $\boldsymbol{x}$ and using the solution for $c_n^{(1)}$ (4.41), so that, rearranging terms, we finally obtain:

$$\frac{\partial c_n^{(0)}}{\partial t} + \nabla_{\boldsymbol{x}} \cdot \left(c_n^{(0)} \left\langle \boldsymbol{u}_n^{(0)} \right\rangle_n - \mathsf{D}_n \nabla_{\boldsymbol{x}} c_n^{(0)} \right) - \tilde{\boldsymbol{u}}_n \cdot \nabla_{\boldsymbol{x}} c_n^{(0)} =$$
$$= r_n c_n^{(0)} - \frac{1}{|\Omega_n|} \int_{\Gamma} \bar{\Phi}_d^{(0)} \, \mathrm{dS}_y, \tag{4.49}$$

$$r_n := \frac{1}{|\Omega_n|} \int_{\Gamma} \boldsymbol{u}_n^{(0)} \cdot \boldsymbol{q} \, \mathrm{dS}_y; \quad \tilde{\boldsymbol{u}}_n := \frac{A_n}{|\Omega_n|} \int_{\Gamma} (\nabla_{\boldsymbol{y}} \boldsymbol{a}) \boldsymbol{q} \, \mathrm{dS}_y, \tag{4.50}$$

$$\mathsf{D}_n := A_n \left(\mathsf{I} - \frac{1}{|\Omega_n|} \int_{\Omega_n} (\nabla_{\boldsymbol{y}} \boldsymbol{a})^{\mathsf{T}} \, \mathrm{d}\boldsymbol{y} \right), \tag{4.51}$$

or, componentwise

$$D_n^{ij} = A_n \left(\delta_{ij} - \frac{1}{|\Omega_n|} \int_{\Omega_n} \frac{\partial a_j}{\partial y_i} \, \mathrm{d}\boldsymbol{y} \right) = A_n \left(\delta_{ij} - \frac{1}{|\Omega_n|} \int_{\Gamma} a_j n_i \, \mathrm{dS}_y \right), \, i, j \in (1, 2, 3).$$

Here, the contributions due to the scalar r_n and the vector $\tilde{\boldsymbol{u}}_n$ can be viewed as effective reaction factor and correction transport velocity, respectively, due to slow modulation of the interface Γ. The second order tensor D_n represents the effective diffusivity tensor for the capillary compartment.

The differential problem given by (4.26,4.35,4.49) (even when (4.19) is used to express $\boldsymbol{u}_n^{(0)}$ as a function of $p_n^{(0)}$) for the capillaries variables $\left\langle \boldsymbol{u}_n^{(0)} \right\rangle_n, c_n^{(0)}, p_n^{(0)}$, is not closed, because the blood and drug fluxes $\bar{\Phi}_b^{(0)}$ and $\bar{\Phi}_d^{(0)}$ depend on the interstitial variables too. Hence, we proceed to derive the macroscale differential system for the interstitial compartment, to write down a closed coupled problem for both interstitial and capillary variables.

4.2. *Interstitial problem*

The interstitial problem (3.4,3.5,3.7,3.10,3.12) for fluid and drug transport in Ω_t, after the two-scales reformulations, reads:

$$\epsilon \boldsymbol{u}_t = -\bar{\kappa} \nabla_{\boldsymbol{y}} p_t - \epsilon \bar{\kappa} \nabla_{\boldsymbol{x}} p_t \quad \text{in } \Omega_t \tag{4.52}$$

$$\nabla_{\boldsymbol{y}} \cdot \boldsymbol{u}_t + \epsilon \nabla_{\boldsymbol{x}} \cdot \boldsymbol{u}_t = 0 \quad \text{in } \Omega_t \tag{4.53}$$

$$\epsilon^2 \frac{\partial c_t}{\partial t} + \nabla_{\boldsymbol{x}} \cdot \left(\epsilon^2 c_t \boldsymbol{u}_n - \epsilon A_n \nabla_{\boldsymbol{y}} c_t - \epsilon^2 A_t \nabla_{\boldsymbol{x}} c_t \right)$$
$$+ \nabla_{\boldsymbol{y}} \cdot \left(\epsilon c_t \boldsymbol{u}_n - A_t \nabla_{\boldsymbol{y}} c_t - \epsilon A_t \nabla_{\boldsymbol{x}} c_t \right) = -\epsilon^2 \bar{h}(c_t) \quad \text{in } \Omega_t \tag{4.54}$$

with interface conditions

$$\left(\epsilon c_t \boldsymbol{u}_t - A_t \nabla_{\boldsymbol{y}} c_t - \epsilon A_t \nabla_{\boldsymbol{x}} c_t \right) \cdot \boldsymbol{n}_t = -\epsilon^2 \bar{\Phi}_d \text{ on } \Gamma \tag{4.55}$$

$$\boldsymbol{u}_t \cdot \boldsymbol{n}_t = -\epsilon \bar{\Phi}_b \text{ on } \Gamma, \tag{4.56}$$

where $\boldsymbol{n}_t = -\boldsymbol{n}$ is the outward unit vector normal to the interstitial surface. Our aim is to determine effective differential equations for the leading order interstitial fields $p_t^{(0)}$, $c_t^{(0)}$, $\left\langle \boldsymbol{u}_t^{(0)} \right\rangle_t$. We start equating coefficients of ϵ^0 in (4.52) to obtain:

$$\nabla_{\boldsymbol{y}} p_t^{(0)} = 0 \rightarrow p_t^{(0)} = p_t^{(0)}(\boldsymbol{x}, t), \tag{4.57}$$

so that the leading order interstitial pressure is locally constant.

Equating coefficients of ϵ^1 in (4.52) and of ϵ^0 in (4.53) and (4.56) we get:

$$\boldsymbol{u}_t^{(0)} = -\bar{\kappa} \nabla_{\boldsymbol{y}} p_t^{(1)} - \bar{\kappa} \nabla_{\boldsymbol{x}} p_t^{(0)} \text{ in } \Omega_t \tag{4.58}$$

$$\nabla_{\boldsymbol{y}} \cdot \boldsymbol{u}_t^{(0)} = 0 \text{ in } \Omega_t \tag{4.59}$$

$$\boldsymbol{u}_t^{(0)} \cdot \boldsymbol{n}_t = 0 \text{ on } \Gamma. \tag{4.60}$$

Now we can substitute relationship (4.58) into (4.59-4.60), such that, since (4.57) applies, we can write the following Laplace problem for $p_t^{(1)}$

$$\nabla_{\boldsymbol{y}}^2 p_t^{(1)} = 0 \text{ in } \Omega_t \tag{4.61}$$

$$\nabla_{\boldsymbol{y}} p_t^{(1)} \cdot \boldsymbol{n}_t = -\nabla_{\boldsymbol{x}} p_t^{(0)} \cdot \boldsymbol{n}_t \text{ on } \Gamma. \tag{4.62}$$

The corresponding compatibility condition

$$\int_{\Gamma} \nabla_{\boldsymbol{x}} p_t^{(0)} \cdot \boldsymbol{n}_t \, \mathrm{dS}_y = 0 \tag{4.63}$$

is satisfied because

$$\int_{\Gamma} \nabla_{\boldsymbol{x}} p_t^{(0)} \cdot \boldsymbol{n}_t \, \mathrm{dS}_y = \int_{\partial \Omega_t} \nabla_{\boldsymbol{x}} p_t^{(0)} \cdot \boldsymbol{n}_t \, \mathrm{dS}_y = \int_{\Omega_t} \nabla_{\boldsymbol{y}} \cdot \nabla_{\boldsymbol{x}} p_t^{(0)} \, \mathrm{d}\boldsymbol{y} = 0, \tag{4.64}$$

where we have used $\boldsymbol{y}$-periodicity and the divergence theorem, as well as the fact that $p_t^{(0)}$ is locally constant (4.57).

Now we exploit the linearity of the problem (4.61)-(4.62) to propose a solution of the form:

$$p_t^{(1)} = -\boldsymbol{P}_t(\boldsymbol{x}, \boldsymbol{y}) \cdot \nabla_{\boldsymbol{x}} p_t^{(0)} + \tilde{p}_t(\boldsymbol{x}), \tag{4.65}$$

where the auxiliary vector $\boldsymbol{P}_t$ solves the following cell problems:

$$\nabla_{\boldsymbol{y}}^2 \boldsymbol{P}_t = 0 \qquad \text{in } \Omega_t \tag{4.66}$$

$$(\nabla_{\boldsymbol{y}} \boldsymbol{P}_t) \boldsymbol{n}_t = \boldsymbol{n}_t \qquad \text{on } \Gamma. \tag{4.67}$$

20   *R. Penta D.Ambrosi A. Quarteroni*

The above system of equations is supplemented by periodicity conditions in $\boldsymbol{y}$ together with suitable uniqueness conditions for $\boldsymbol{P}_t$. For example we can impose:

$$\langle \boldsymbol{P}_t \rangle_t = \boldsymbol{0}. \tag{4.68}$$

An integral averaging of (4.58) over Ω_t provides the macroscale equation for the velocity in the tumor interstitium,

$$\left\langle \boldsymbol{u}_t^{(0)} \right\rangle_t = -\bar{\kappa} \mathsf{E} \nabla_{\boldsymbol{x}} p_t^{(0)}, \tag{4.69}$$

where the second order tensor E is defined by:

$$\mathsf{E} := \mathsf{I} - \frac{1}{|\Omega_t|} \int_{\Omega_t} (\nabla_y \boldsymbol{P}_t)^{\mathsf{T}} \, \mathrm{d}\boldsymbol{y}, \tag{4.70}$$

or, in component notation:

$$E_{ij} = \delta_{ij} - \frac{1}{|\Omega_t|} \int_{\Omega_t} \frac{\partial P_t^j}{\partial y_i} \, \mathrm{d}\boldsymbol{y} = \delta_{ij} + \frac{1}{|\Omega_t|} \int_{\Gamma} P_t^j n_i \, \mathrm{d}\mathsf{S}_y. \tag{4.71}$$

Also in the interstitial compartment, the average velocity profile is therefore given by an anisotropic Darcy's law. Then, the whole system can be viewed as a double porous medium on the macroscale. As before, the role of the microstructure is encoded in the permeability tensor, which is given by E in the tissue interstitium. To close the entire macroscale model, we need a macroscale equation for the leading order interstitial pressure $p_t^{(0)}$ and the drug concentration $c_t^{(0)}$. We recognize that the interstitial relationships (4.53-4.56) are formally analogous to equations (4.7-4.10), provided that the following identifications are made:

$$\boldsymbol{u}_n \to \boldsymbol{u}_t; \quad c_n \to c_t; \quad \bar{\Phi}_b \to -\bar{\Phi}_b; \quad \bar{\Phi}_d \to -\bar{\Phi}_d; \quad \frac{\partial c_n}{\partial t} \to \frac{\partial c_t}{\partial t} + \bar{h}(c_t); \quad A_n \to A_t;$$

$$|\Omega_n| \to |\Omega_t| \tag{4.72}$$

and

$$\boldsymbol{n} \to \boldsymbol{n}_t = -\boldsymbol{n}. \tag{4.73}$$

By applying in the interstitial compartment the same asymptotic analysis previously carried out for the capillary compartment in equations (4.7-4.10) to (4.53-4.56), we obtain the macroscale equations (of the form (4.35), (4.49)):

$$-\nabla_{\boldsymbol{x}} \cdot \left\langle \boldsymbol{u}_t^{(0)} \right\rangle_t = \nabla_{\boldsymbol{x}} \cdot \left(\bar{\kappa} \mathsf{E} \nabla_{\boldsymbol{x}} p_t^{(0)} \right) = -\frac{1}{|\Omega_t|} \int_{\Gamma} (\bar{\Phi}_b^{(0)} - \boldsymbol{u}_n^{(0)} \cdot \boldsymbol{q}) \, \mathrm{d}\mathsf{S}_y. \tag{4.74}$$

and

$$\frac{\partial c_t^{(0)}}{\partial t} + \nabla_{\boldsymbol{x}} \cdot \left(c_t^{(0)} \left\langle \boldsymbol{u}_t^{(0)} \right\rangle_t - \mathsf{D}_t \nabla_{\boldsymbol{x}} c_t^{(0)} \right) - \tilde{\boldsymbol{u}}_t \cdot \nabla_{\boldsymbol{x}} c_t^{(0)} =$$
$$= r_t c_t^{(0)} + \frac{1}{|\Omega_t|} \int_{\Gamma} \bar{\Phi}_d^{(0)} \, \mathrm{d}\mathsf{S}_y - \bar{h}(c_t^{(0)}), \tag{4.75}$$

where

$$r_t := -\frac{1}{|\Omega_t|} \int_\Gamma \boldsymbol{u}_t^{(0)} \cdot \boldsymbol{q} \; \mathrm{dS}_y; \quad \tilde{\boldsymbol{u}}_t := -\frac{A_t}{|\Omega_t|} \int_\Gamma (\nabla_{\boldsymbol{y}} \boldsymbol{b}) \boldsymbol{q} \; \mathrm{dS}_y \tag{4.76}$$

$$\mathsf{D}_t := A_t \left(\mathsf{I} - \frac{1}{|\Omega_t|} \int_{\Omega_t} (\nabla_{\boldsymbol{y}} \boldsymbol{b})^{\mathsf{T}} \; \mathrm{d}\boldsymbol{y} \right), \tag{4.77}$$

or, componentwise

$$D_t^{ij} = A_t \left(\delta_{ij} - \frac{1}{|\Omega_t|} \int_{\Omega_t} \frac{\partial b_j}{\partial y_i} \; \mathrm{d}\boldsymbol{y} \right) = A_t \left(\delta_{ij} + \frac{1}{|\Omega_t|} \int_\Gamma b_j n_i \; \mathrm{dS}_y \right), \quad i,j \in (1,2,3).$$

The auxiliary vector $\boldsymbol{b}(\boldsymbol{x}, \boldsymbol{y})$ solves the cell problem (4.42-4.43) in the interstitial domain, namely:

$$\nabla_{\boldsymbol{y}}^2 \boldsymbol{b} = 0 \quad \text{in } \Omega_t \tag{4.78}$$

$$(\nabla_{\boldsymbol{y}} \boldsymbol{b}) \boldsymbol{n}_t = \boldsymbol{n}_t \quad \text{on } \Gamma, \tag{4.79}$$

where, again, a further condition for $\boldsymbol{b}$ is required to ensure uniqueness, for example

$$\langle \boldsymbol{b} \rangle_t = \boldsymbol{0}. \tag{4.80}$$

4.3. *Main result and discussion*

The system of equations (4.35,4.26,4.49,4.74,4.69,4.75) represents the effective differential model for the leading order average pressure, velocity and concentration fields $p_n^{(0)}$, $\left\langle \boldsymbol{u}_n^{(0)} \right\rangle_n$, $c_n^{(0)}$, $p_t^{(0)}$, $\left\langle \boldsymbol{u}_t^{(0)} \right\rangle_t$ $c_t^{(0)}$, which describe the macroscopic behavior of the fluid and drug dynamics in vascularized tissues. Summarizing, the resulting equations in non-conservative form are

$$\begin{cases} \dfrac{\partial c_n^{(0)}}{\partial t} + \left(\left\langle \boldsymbol{u}_n^{(0)} \right\rangle_n - \tilde{\boldsymbol{u}}_n \right) \cdot \nabla_{\boldsymbol{x}} c_n^{(0)} - \nabla_{\boldsymbol{x}} \cdot \left(\mathsf{D}_n \nabla_{\boldsymbol{x}} c_n^{(0)} \right) = -\mathcal{R}_n[c_n^{(0)}] & (4.81) \\[2ex] \dfrac{\partial c_t^{(0)}}{\partial t} + \left(\left\langle \boldsymbol{u}_t^{(0)} \right\rangle_t - \tilde{\boldsymbol{u}}_t \right) \cdot \nabla_{\boldsymbol{x}} c_t^{(0)} - \nabla_{\boldsymbol{x}} \cdot \left(\mathsf{D}_t \nabla_{\boldsymbol{x}} c_t^{(0)} \right) = -\mathcal{R}_t[c_t^{(0)}] & (4.82) \\[2ex] \nabla_{\boldsymbol{x}} \cdot \left(\mathsf{K} \nabla_{\boldsymbol{x}} p_n^{(0)} \right) = \dfrac{S}{|\Omega_n|} \bar{\Phi}_b^{(0)} - \dfrac{1}{|\Omega_n|} \int_\Gamma \boldsymbol{u}_n^{(0)} \cdot \boldsymbol{q} \; \mathrm{dS}_y & (4.83) \\[2ex] \nabla_{\boldsymbol{x}} \cdot \left(\bar{\kappa} \mathsf{E} \nabla_{\boldsymbol{x}} p_t^{(0)} \right) = -\dfrac{S}{|\Omega_t|} \bar{\Phi}_b^{(0)} + \dfrac{1}{|\Omega_t|} \int_\Gamma \boldsymbol{u}_t^{(0)} \cdot \boldsymbol{q} \; \mathrm{dS}_y & (4.84) \\[2ex] \left\langle \boldsymbol{u}_n^{(0)} \right\rangle_n = -\mathsf{K} \nabla_{\boldsymbol{x}} p_n^{(0)} & (4.85) \\[2ex] \left\langle \boldsymbol{u}_t^{(0)} \right\rangle_t = -\bar{\kappa} \mathsf{E} \nabla_{\boldsymbol{x}} p_t^{(0)}, & (4.86) \end{cases}$$

where $\mathsf{E}(\boldsymbol{x})$, $\mathsf{K}(\boldsymbol{x})$, $\mathsf{D}_t(\boldsymbol{x})$, $\mathsf{D}_n(\boldsymbol{x})$ are the effective hydraulic conductivity and diffusion tensors, $|\Omega_n|(\boldsymbol{x})$, $|\Omega_t|(\boldsymbol{x})$ are the capillary network and interstitial cell volume fractions. We recall the definition of the vector $\boldsymbol{q}$ given by (4.34) in terms of the interface position vector $\boldsymbol{r}(\boldsymbol{x}, \boldsymbol{y})$:

$$\boldsymbol{q} := (\nabla_{\boldsymbol{x}} \boldsymbol{r}(\boldsymbol{x}, \boldsymbol{y}))^{\mathsf{T}} \boldsymbol{n}.$$

The reaction operators $\mathcal{R}_n$ and $\mathcal{R}_t$ are defined as:

$$\mathcal{R}_n[c_n^{(0)}] := \frac{S}{|\Omega_n|}\bar{\Phi}_d^{(0)} + c_n^{(0)}\nabla_{\boldsymbol{x}} \cdot \left\langle \boldsymbol{u}_n^{(0)} \right\rangle_n - r_n c_n^{(0)} \tag{4.87}$$

$$\mathcal{R}_t[c_t^{(0)}] := -\frac{S}{|\Omega_t|}\bar{\Phi}_d^{(0)} + c_t^{(0)}\nabla_{\boldsymbol{x}} \cdot \left\langle \boldsymbol{u}_t^{(0)} \right\rangle_t - r_t c_t^{(0)} + \bar{h}(c_t^{(0)}). \tag{4.88}$$

Since the blood flux $\bar{\Phi}_b^{(0)}$ and the drug flux $\bar{\Phi}_d^{(0)}$ (given by (4.32,4.47) when a complete Kedem-Katchalsky formulation is assumed) and the reaction function $\bar{h}$ depend on $p_n^{(0)}$, $p_t^{(0)}$, $c_n^{(0)}$, $c_t^{(0)}$ only, then they are also $\boldsymbol{y}$-constant and

$$S(\boldsymbol{x}) = \int_\Gamma \mathrm{dS}_y \tag{4.89}$$

is the unit cell capillary walls surface. The system (4.81-4.86) provides a closed homogenized model for the leading order macroscale variables, as the non-averaged fields $\boldsymbol{u}_n^{(0)}$ and $\boldsymbol{u}_t^{(0)}$ which explicitly appear in (4.83,4.84) and also in the effective reactions r_n and r_t defined in (4.50,4.76), can be expressed as functions of $p_n^{(0)}$ and $p_t^{(0)}$ only as follows:

$$\boldsymbol{u}_n^{(0)} = -\mathsf{W}\nabla_{\boldsymbol{x}}p_n^{(0)} \tag{4.90}$$

$$\boldsymbol{u}_t^{(0)} = -\bar{\kappa}\left(\mathsf{I} - (\nabla_{\boldsymbol{y}}\boldsymbol{P}_t)^\mathsf{T}\right)\nabla_{\boldsymbol{x}}p_t^{(0)}, \tag{4.91}$$

where we exploited (4.19) and (4.58,4.65), respectively.

The fluid dynamics is described by the double porous medium model (4.85,4.86), with mass exchange between compartments, due to both the blood leakage and by the effective mass flux driven by spatial heterogeneities, at the right hand sides of (4.83-4.84).

The drug dynamics is described by the advection-diffusion-reaction model (4.81-4.82). Both the interstitial and the capillary advection are due to the corresponding fluid flow, up to a correction factor that accounts for possible lack of macroscopic uniformity in the system. The reaction operators (4.87-4.88) encode the drug exchange between the two compartments, the influence of the blood leakage on the drug dynamics and the effective reaction related to macroscopic changes of the microstructure. Chemical reactions occuring in the interstitium are also taken into account.

The whole model holds over the macroscale, where the difference between interstitial and capillary compartment is immaterial. Nevertheless, the role of the microstructure can be understood in the model, as the cell volumes fractions $|\Omega_n|(\boldsymbol{x})$, $|\Omega_t|(\boldsymbol{x})$ and interface area $S(\boldsymbol{x})$ appear explicitly. Furthermore, the macroscale hydraulic conductivity and diffusion tensors $\mathsf{E}(\boldsymbol{x})$, $\mathsf{K}(\boldsymbol{x})$, $\mathsf{D}_t(\boldsymbol{x})$, $\mathsf{D}_n(\boldsymbol{x})$ defined by (4.70,4.27,4.51, 4.77), can be obtained after solving the cell problems (4.66-4.67), (4.21-4.24), (4.78-4.79), (4.42-4.43), respectively.

The unit cell geometry is needed to compute contributions that account for macroscopic changes of the microstructure (i.e. any term including the vector $\boldsymbol{q}$, defined in

(4.34)). We summarize the steps needed to compute the solution of the differential problem (4.81-4.86) as follows:

(1) Given a macroscale domain $\Omega_H \subset \mathbb{R}^3$ and a time interval $(0, T)$, $T \in \mathbb{R}^+$, fix suitable initial conditions in Ω_H and provide boundary conditions on $\partial\Omega_H$.

(2) Define the cell geometry as a function of $\boldsymbol{x}$, such that, in particular, $|\Omega_n|(\boldsymbol{x})$, $|\Omega_t|(\boldsymbol{x})$, $S(\boldsymbol{x})$ and $\boldsymbol{r}(\boldsymbol{x}, \boldsymbol{y})$ are prescribed.

(3) Prescribe material properties to get the proper non-dimensional numbers as defined in (3.16). According to the specific physical system at hand, choose the proper functional form of the fluid and drug fluxes and interstitial reaction to get $\bar{\Phi}_b^{(0)}$, $\bar{\Phi}_d^{(0)}$ and $\bar{h}(c_t^{(0)})$.

(4) For every $\boldsymbol{x} \in \Omega_H$, solve the cell problems (4.66-4.67), (4.21-4.24), (4.78-4.79), (4.42-4.43) to compute the auxiliary cell variables $\boldsymbol{P}_t$, W, $\boldsymbol{b}$, $\boldsymbol{a}$.

(5) Compute the correction velocities $\tilde{\boldsymbol{u}}_n$, $\tilde{\boldsymbol{u}}_t$ and the macroscale coefficients encoded in the effective tensors E, K, D_t, D_n, using definitions (4.50),(4.76), (4.70,4.27,4.51, 4.77), respectively.

(6) For every $\boldsymbol{x} \in \Omega_H$ and for every $t \in (0, T)$, solve the differential problem (4.81-4.86), equipped with the macroscale boundary and interface conditions prescribed in step (1), to obtain $p_n^{(0)}$, $\left\langle \boldsymbol{u}_n^{(0)} \right\rangle_n$, $c_n^{(0)}$, $p_t^{(0)}$, $\left\langle \boldsymbol{u}_t^{(0)} \right\rangle_t$, $c_t^{(0)}$.

Remark 4.2. Note that the mathematical model we obtained can be discretized on a coarse "macro" computational grid, while the relevant physical phenomena are now captured on the tissue scale. A numerical solution of the original problem (3.2-3.12) would require an extremely fine grid to capture the detail of the microstructure, which is characterized by the intercapillary distance d. Instead, as the effective governing equations (4.81-4.86) are to be solved on the macroscale, a much coarser grid can be used. The role of the microstructure is now encoded in standard differential cell problems, to be solved for every macroscale computational node (see figure 1). Finally, whenever macroscopic uniformity applies, the representative cell does not depend on the macroscale any longer, and an average representative radius for the capillaries can be fixed. In this particular case, the system dramatically simplifies, as every correction factor due to macroscopic changes of the microstructure (i.e including the vector $\boldsymbol{q}$) vanishes, the cell problems depend on the microscale $\boldsymbol{y}$ only and they are to be solved once for every $\boldsymbol{x} \in \Omega_H$, to give the constant macroscale coefficients E,K,D_n,D_t.

4.3.1. *Comparison with the model proposed by Shipley & Chapman [49]*

The fluid and drug transport model reported in [49] can be obtained as a particular case of (4.81-4.86), under the following simplifying assumptions:

(1) Macroscopic uniformity, i.e. the microstructure is unique; hence $\boldsymbol{q} = 0$, and r_n, r_t, $\tilde{\boldsymbol{u}}_n$, $\tilde{\boldsymbol{u}}_t$ vanish. $|\Omega_n|$, $|\Omega_t|$, S are simply constant numbers.

(2) Fluid flow in the capillaries is assumed as Newtonian, i.e. $\bar{\mu}$ is constant.

(3) Diffusion is negligible compared to advection, i.e. A_n, $A_t \to 0$, hence the macroscale diffusivity contribution is neglected.

(4) The Starling's law for the blood flux neglects the osmotic pressure drop due to the drug concentration and a relationship of the type $\phi_b = L_p(p_n - p_t)$ is chosen. As a result, we obtain:

$$\bar{\Phi}_b^{(0)} = \bar{L}_p \left(p_n^{(0)} - p_t^{(0)} \right), \tag{4.92}$$

where

$$\bar{L}_p = \frac{L_p L^2 \mu}{d^3} \tag{4.93}$$

is the non-dimensional vessel conductivity. In this case, the fluid and drug dynamics are decoupled, as the solution for the fluid variables does not depend on the interstitial and capillary concentrations any longer.

(5) The membrane law for the drug flux ignores the advection of macromolecules across the interface and a relationship of the type $\phi_d = P(c_n - c_t)$ is chosen, leading to:

$$\bar{\Phi}_d^{(0)} = \bar{\Upsilon} \left(c_n^{(0)} - c_t^{(0)} \right), \tag{4.94}$$

where

$$\bar{\Upsilon} = \frac{P \mu L}{C d^3} \tag{4.95}$$

is the non-dimensional diffusive permeability of the capillary walls.

(6) Linear uptake in the interstitium, that is $h(c_t) = \gamma c_t$ and

$$\bar{h}(c_t^{(0)}) = \overline{\mathrm{Da}} c_t^{(0)}, \tag{4.96}$$

where $\overline{\mathrm{Da}}$ is the Damkohler number given by:

$$\overline{\mathrm{Da}} = \frac{\gamma L \mu}{C d^2}. \tag{4.97}$$

Whenever the above simplifying assumptions hold, the system (4.81-4.86), in conservative form, reduces to:

$$\begin{cases} \dfrac{\partial c_n^{(0)}}{\partial t} + \nabla_{\boldsymbol{x}} \cdot \left(c_n^{(0)} \left\langle \boldsymbol{u}_n^{(0)} \right\rangle_n \right) = -\dfrac{S\bar{\Upsilon}}{|\Omega_n|}(c_n^{(0)} - c_t^{(0)}) & (4.98) \\[3mm] \dfrac{\partial c_t^{(0)}}{\partial t} + \nabla_{\boldsymbol{x}} \cdot \left(c_t^{(0)} \left\langle \boldsymbol{u}_t^{(0)} \right\rangle_t \right) = \dfrac{S\bar{\Upsilon}}{|\Omega_t|}(c_n^{(0)} - c_t^{(0)}) - \overline{\mathrm{Da}}c_t^{(0)} & (4.99) \\[3mm] \nabla_{\boldsymbol{x}} \cdot \left(\mathsf{K}\nabla_{\boldsymbol{x}}p_n^{(0)} \right) = \dfrac{S}{|\Omega_n|}\bar{L}_p(p_n^{(0)} - p_t^{(0)}) & (4.100) \\[3mm] \nabla_{\boldsymbol{x}} \cdot \left(\bar{\kappa}\mathsf{E}\nabla_{\boldsymbol{x}}p_t^{(0)} \right) = -\dfrac{S}{|\Omega_t|}\bar{L}_p(p_n^{(0)} - p_t^{(0)}) & (4.101) \\[3mm] \left\langle \boldsymbol{u}_n^{(0)} \right\rangle_n = -\mathsf{K}\nabla_{\boldsymbol{x}}p_n^{(0)} & (4.102) \\[3mm] \left\langle \boldsymbol{u}_t^{(0)} \right\rangle_t = -\bar{\kappa}\mathsf{E}\nabla_{\boldsymbol{x}}p_t^{(0)}. & (4.103) \end{cases}$$

Equations of the form (4.98-4.103) have been derived by [49] for the fluid and drug transport in vascularized tissues (up to notation issues). The cell problems related to the solutions for the effective hydraulic conductivity tensors K and E, given by (4.21-4.24) and (4.66-4.67), respectively, are exactly the same introduced above and the same is true for the several related non-dimensional numbers, even though in [49] a different scaling approach is performed. In fact, accounting for relationships (2.30), (3.19) and (3.16), the non-dimensional numbers appearing in (4.98-4.103) can be equivalently rewritten as

$$\bar{\Upsilon} = \frac{PL}{Ud}, \quad \overline{\mathrm{Da}} = \frac{\gamma L}{U}, \quad \bar{L}_p = \frac{L_p L^2 \mu}{d^3}, \quad \bar{\kappa} = \frac{k}{d^2}, \tag{4.104}$$

such that, in our notation, they are defined exactly the same way as their corresponding counterparts in [49][a].

Remark 4.3. Equations (4.100-4.103) exactly match the double porous medium model in [49], whereas (4.98-4.99) agree with one of the drug dynamics model derived by the authors [b], where the interstitial and capillary concentrations can be tracked independently. It is worth remarking that their derivation adopts a different viewpoint, as every non-dimensional number in their formulation is scaled with respect to ϵ on the basis of an *a priori* order of magnitude estimate. It is worth noting that assumption (3) is not exploited by the authors; diffusion plays a role in the derivation of their model, but does not appear at leading order. Furthermore, they discuss different types of interface conditions, including the membrane law, continuity, and jump between the interstitial and capillary concentrations across the capillary walls. As a result, they do not obtain a unique formulation for the

---

[a]Up to notation issues; indeed, in [49] the diffusive permeability of the membrane P, the reaction uptake rate γ and the non-dimensional vessels conductivity $\bar{L}_p$ are denoted by r, λ and $\bar{R}$ respectively.
[b]Page 1484, paragraph 3.2.4, [49].

drug dynamics, rather, several different options are presented. Nevertheless, the resulting models can be viewed as either particular or limiting cases of equations of the type (4.98-4.99), as reported in [48].

5. Conclusions

In this work we have considered a system of partial differential equations (in non-dimensional form) that expresses the balance laws (3.2-3.7) between the fluid and drug transport in the tumor interstitium and its embedded microvasculature. The flow coupling across the capillary walls has been enforced by the interface conditions (3.8-3.12), which account for blood and drug transcapillary exchange across the vessels walls. By exploiting the strong spatial scale separation between the tumor characteristic length and the mean intercapillary distance, we obtained a closed differential problem for the leading order quantities $p_n^{(0)}$, $p_t^{(0)}$, $c_n^{(0)}$, $c_t^{(0)}$, $\left\langle \boldsymbol{u}_n^{(0)} \right\rangle_n$, $\left\langle \boldsymbol{u}_t^{(0)} \right\rangle_t$ on the tissue scale, by means of the homogenization technique, under the assumption of local periodicity only; macroscopic variations of the microstructure are therefore allowed.

According to the resulting system of equations, the fluid flow obeys a double porous medium model, where the effective hydraulic conductivity tensors can be computed solving standard differential cell problems. Mass sources contributions account for both the effective transport between the capillary and interstitial compartments and macroscopic changes of the microvasculature.

The effective governing equations for drug transport comprise a double generalized advection-diffusion-reaction model, where the reaction operators account for the transvascular exchange of drug across the capillary walls, as well as the influence of the blood transfer and slow modulation of the microvasculature geometry. Chemical reactions which might occur in the tumor interstitium are also taken into account. The role of the microstructure is also encoded in the effective diffusivity tensors, which can be computed by solving classical differential cell problems on a single unit cell.

Our main result has been the derivation of a mathematical model that retains the most relevant physical phenomena of the system at the tissue scale: the role of the microvasculature is recovered via the effective macroscale coefficients of the model, which can be calculated solving standard differential problems on a single cell for every macroscale point $\boldsymbol{x}$. Moreover, an interesting feature of our model is its computational convenience.

The mathematical model reported in [49] can be recovered under a number of simplifying assumptions. Remarkable differences are that diffusion plays here a role at the tissue scale, and the interplay between fluid and drug transport is accounted for, via a general Kedem-Katchalsky model for the interface fluxes. The osmotic pressure due to the difference in drug concentrations is retained, yielding a coupling between blood and drug dynamics. Furthermore, we also allow macroscopic varia-

tions of the microstructure and compute the arising effective velocities, reactions and fluxes. In general, the main contribution of the current work is in addressing more generality in the physics of the biological system, in terms of a fully non-equilibrium, non-linear formulation for the blood and drug interplay, together with possibly non-linear reactions that might occur in the tissue. The effective governing equations do not depend explicitly on specific physical regimes: however, simplified cases can be obtained performing an *a posteriori* estimate of the non-dimensional numbers, depending on the actual system at hand. Finally, local periodicity only is assumed, and the present model still applies when spatial heterogeneities, which often occur in tumor vasculatures, appear.

Nevertheless, some simplifying assumptions are enforced. In particular, we did not account for a fully non-Newtonian rheology of the blood, even though (slow) variations of the relative viscosity with respect to the effective capillary radius are allowed. The microstructure can vary over the macroscale, but is fixed in time, such that we do not account for adaptation or re-modelling issues (see for example [40, 34]). The elastic deformability of the porous structure is neglected, even though for a certain class of tissues, the elastic (or visco-elastic) properties of the porous solid mass cannot be ignored. In this scenario, it has been shown that the hydraulic conductivity of the tissue depends also on the tissue strains [30], and poroelastic modeling approaches with anisotropic dependence of the hydraulic conductivity upon tissue deformation have been recently explored [5].

This work represents a first attempt to test both the impact of the vascular geometry and the influence of drug parameters on the tumor fluid dynamics. This mathematical framework can be exploited to simulate numerically the fluid and drug transport coupling on real tumor geometries extracted from medical images. Numerical results can be compared to clinical data to achieve validation whereas, in the long term, predictions from this model could help to improve anti-cancer strategies.

Acknowledgments

References

1. D Ambrosi and L Preziosi. On the closure of mass balance models for tumor growth. *Math. Mod. Meth. Appl. Sci.*, 12:737, 2002.
2. T Arbogast and HL Lehr. Homogenization of a darcy-stokes system modeling vuggy porous media. *Computational Geosciences*, 10:291–302, 2006.

28 *REFERENCES*

3. GS Beavers and DD Joseph. Boundary conditions at a naturally permeable wall. *Journal of Fluid Mechanics*, 30:197–207, 1967.

4. G Bhalla and WM Deen. Effects of molecular shape on osmotic reflection coefficients. *Journal of Membrane Science*, 306:116–124, 2007.

5. A Bottaro and T Ansaldi. On the infusion of a therapeutic agent into a solid tumor modeled as a poroelastic medium. *Journal of Biomechanical engineering*, 134:1–6, 2012.

6. Y Boucher, LT Baxter, and RK Jain. Interstitial pressure gradiennts in tissue-isolated and subcutaneous tumors: implications for therapy. *Cancer Research*, 50:4478–4484, 1990.

7. R Burridge and J Keller. Poroelasticity equations derived from microstructure. *Journal of acoustical society of America*, 70:1140–1146, 1981.

8. P Carmeliet and RK Jain. Angiogenesis in cancer and other diseases. *Nature*, 407:249–257, 2000.

9. B M Cooke and J Stuart. Automated measurements of plasma viscosity by a capillary viscometer. *Journal of clinical pathology*, 41:1213–1216, 1988.

10. M Discacciati and A Quarteroni. Navier-stokes/darcy coupling: modeling, analysis, and numerical approximation. *Revista Matemática Complutense*, 22(2):315–426, 2009.

11. MR Dreher, W Liu, CR Michelic, MW Dewhirst, F Yuan, and A Chilkoti. Tumor vascular permability, accumulation and penetration of macromolecular drug carriers. *JNCI*, 98:335–344, 2006.

12. R Fahareus and T Lindqvist. The viscosity of the blood in narrow capillary tubes. *American Journal of Physiology*, 96:562–568, 1931.

13. L Formaggia, A Quarteroni, and A Veneziani. *Cardiovascular Mathematics*. Springer, 2009.

14. H Hashizume. Openings between defective endothelial cells explain tumor vessel leakiness. *Am. J. Pathol.*, 156:1363–1380, 2000.

15. C Heldin, K Rubin, K Pietras, and A Ostman. High interstitial fluid pressure-an obstacle in cancer therapy. *Nature Reviews Cancer*, 4:806–813, 2004.

16. M Holmes. *Introduction to perturbation method.* Springer-Verlag, 1995.

17. U Hornung. *Homogenization and Porous Media. Interdisciplinary Applied Mathematics, vol. 6.* Springer-Verlag, New York, 1997.

18. W Jäger, A Mikelić, and M Neuss-Radu. Analysis of differential equations modelling the reactive flow through a deformable system of cells. *Archive for rational mechanics and analysis*, 192(2):331–374, 2009.

19. W Jäger, A Mikelic, and M Neuss-Radu. Homogenization limit of a model system for interaction of flow, chemical reactions, and mechanics in cell tissues. *SIAM Journal on Mathematical Analysis*, 43(3):1390–1435, 2011.

20. RK Jain. Transport of molecules across tumor vasculature. *Cancer Metastasis Review*, 6:559–594, 1987.

21. RK Jain. Determinants of tumor blood flow: A review. *Cancer Research*, 48:2641–2658, 1988.

22. RK Jain and LT Baxter. Mechanisms of heterogeneous distribution of mono-clonal antibodies and other macromolecules in tumors: significance of elevated interstitial pressure. *Cancer Research*, 48:7022–7032, 1988.

23. RK Jain, RT Tong, and LL Munn. Effect of vascular normalization by antian-giogenic therapy on interstitial hypertension, peritumor edema, and lymphatic metastasis: insights from a mathematical model. *Cancer Res*, 67(6):2729–2735, Mar 2007.

24. A R Jayaweera, N Edwards, W P Glasheen, F S Villanueva, R D Abbott, and S Kaul. In vivo myocardial kinetics of air-filled albumin microbubbles during myocardial contrast ecocardiography. comparison with radiolabeled red blood cells. *Circulation Research*, 74:1157–1165, 1994.

25. IP Jones. Low reynolds number flow past a porous spherical shell. *Mathematical Proceedings of the Cambridge Philosofical Society*, 73:231–238, 1973.

26. O Kedem and A Katchalsky. Thermodynamic of the permeability of biological membranes to non-electrolytes. *Biochimica and Biophysica Acta*, 27:229–246, 1958.

27. JR Less, TC Skalak, and EM Sevick. Microvascular architecture in a mam-mary carcinoma: Branching patterns and vessels dimensions. *Cancer Research*, 51:265–273, 1991.

28. S Modok, P Hyde, H Mellor, T Roose, and R Callaghan. Diffusivity and dis-tribution of vinblastine in three-dimensional tumour tissue: Experimental and mathematical modelling. *European Journal of Cancer*, 42:2404–2413, 2006.

29. S Modok, R Scott, R Alderden, M Hall, H Mellor, S Bohic, T Roose, T Ham-bley, and R Callaghan. Transport kinetics of four-and six-coordinate platinum compounds in the multicell layer tumour model. *British Journal of Cancer*, 97:194–200, 2007.

30. PA Netti, DA Berk, MA Swartz, AJ Grodzinsky, and RK Jain. Role of ex-tracellular matrix assembly in interstitial transport in solid tumors. *Cancer Research*, 60:2497–2503, 2000.

31. M Neuss-Radu and W Jäger. Effective transmission conditions for reaction-diffusion processes in domains separated by an interface. *SIAM Journal on Mathematical Analysis*, 39(3):687–720, 2007.

32. J Tinsley Oden, Andrea Hawkins, and Serge Prudhomme. General diffuse-interface theories and an approach to predictive tumor growth modeling. *Math-ematical Models and Methods in Applied Sciences*, 20(03):477–517, 2010.

33. JT Oden, K Vemaganti, and N Moës. Hierarchical modeling of heterogeneous solids. *Computer Methods in Applied Mechanics and Engineering*, 172(1):3–25, 1999.

34. MR Owen, T Alarcon, PK Maini, and HM Byrne. Angiogenesis and vascular remodelling in normal and cancerous tissues. *Journal of Mathematical Biology*, 58:689–721, 2008.

35. R Penta, D Ambrosi, and RJ Shipley. Effective governing equations for poroe-lastic growing media. *The Quarterly Journal of Mechanics and Applied Math-*

ematics, 67(1):69–91, 2014.

36. C Pozrikidis. Numerical simulations of blood flow through microvascular capillary networks. *Bullettin of Mathematical Biology*, 71:1520–1541, 2009.

37. L Preziosi and HM Byrne. Modelling solid tumour growth using the theory of mixtures. *Math. Med. Biol.*, 20:341–366, 2003.

38. A R Pries, T W Secomb, P Gaehtgens, and J F Gross. Blood flow in microvascular networks. experiments and simulations. *Circulation Research*, 67:826–834, 1990.

39. AR Pries, D Neuhaus, and P Gaehtgens. Blood viscosity in tube flow: dependence on diameter and hematocrit. *American Journal of Physiology-Heart and Circulatory Physiology*, 263(6):H1770–H1778, 1992.

40. AR Pries, TW Secomb, and P Gaehtgens. Structural adaptation and stability of microvascular networks: theory and simulations. *American Journal of physiology*, 275:349–360, 1998.

41. KR Rajagopal. On a hierarchy of approximate models for flows of incompressible fluids through porous solids. *Mathematical Models and Methods in Applied Sciences*, 17(02):215–252, 2007.

42. PW Rand, E Lacombe, and HE Hunt. Viscosity of normal human blood under normothermic and hypothermic conditions. *Journal of Applied Physiology*, 19:117–122, 1964.

43. A Romkes, JT Oden, and K Vemaganti. Multi-scale goal-oriented adaptive modeling of random heterogeneous materials. *Mechanics of materials*, 38(8):859–872, 2006.

44. E Sanchez-Palencia. *Non-Homogeneous Media and Vibration Theory-Lecture Notes in Physics 127*. Springer-Verlag, Berlin, Germany, 1980.

45. MM Schuff, JP Gore, and EA Nauman. A mixture theory model of fluid and solute transport in the microvasculature of normal and malignant tissues. i. theory. *Journal of Mathematical Biology*, 66:1179–1207, 2013.

46. MM Schuff, JP Gore, and EA Nauman. A mixture theory model of fluid and solute transport in the microvasculature of normal and malignant tissues. ii. factor sensitivity analysis, calibration, and validation. *Journal of Mathematical Biology*, in press:1–31, 2013.

47. A Scomparin, S Salmaso, S Bersani, R Satchi-Fainaro, and P Caliceti. Novel folated and non-folated pullulan bioconjugates for anticancer drug delivery. *European Journal of Pharmaceutical Sciences*, 42:547–558, 2011.

48. R Shipley. *Multiscale Modelling of Fluid and Drug Transport in Vascular Tumors*. PhD thesis, St. Hugh's College University of Oxford, 2008.

49. RJ Shipley and J Chapman. Multiscale modelling of fluid and drug transport in vascular tumors. *Bulletin of Mathematical Biology.*, 72:1464–1491, 2010.

50. M Simonescu, N Simonescu, and GE Palade. Morphometric data on the endothelium of blood capillaries. *The Journal of cell biology*, 60:128–152, 1974.

51. CW Stevens, RF Munden, KM Forster, JF Kelly, L Liao, G Starkschall,

S Tucker, and R Komaki. Respiratory driven lung tumor motion is indipendent of tumor size, tumor location and pulmonary function. *International Journal of Radiation Oncology*Biology*Physics*, 51:62–68, 2001.

52. EA Swabb, J Wei, and PM Gullino. Diffusion and convection in normal and neoplastic tissues. *Cancer Research*, 34:2814–2822, 1974.

53. Lei Tang, Jing Su, De-Shuang Huang, Daniel Y. Lee, King C. Li, and Xiaobo Zhou. An integrated multiscale mechanistic model for cancer drug therapy. *ISRN Biomathematics*, 2012:12, 2012.

54. J Waniewsky. Mathematical modeling of fluid and solute transport in hemodyalisis and peritoneal analysis. *Journal of Membrane Science*, 274:24–37, 2006.

55. TI Zohdi, JT Oden, and GJ Rodin. Hierarchical modeling of heterogeneous bodies. *Computer Methods in Applied Mechanics and Engineering*, 138(14):273 – 298, 1996.